
FIELD TRIP GUIDE

19 – 21 May (Pre-conference)
24 – 26 May (Post-conference)

The Maures-Tanneron Massif – Day 1 (May 19)

Michel Corsini and Julie Schneider

1. Geological setting

The Maures-Tanneron massif (MTM) forms a part of the Crystalline Provence (Fig. 1-1), which constitutes one of the southernmost segments of the Variscan belt in France located near the Mediterranean Sea [Matte, 2001]. This segment of Paleozoic crust is mainly composed of highgrade metamorphic rocks intruded by Carboniferous granitoids.

1.1. Structural pattern

The major faults and fold structures of the MTM display a submeridian trend (Figs. 1). Regarding the metamorphic grade of rocks and the style of deformation, the MTM is subdivided into two main domains, representing different crustal levels separated by the Joyeuse-Grimaud fault:

- the eastern domain is representative of a deep-crustal level, marked by granulite/amphibolite facies metamorphism, associated with pervasive melting. This domain exhibits migmatites crosscut by several generations of synorogenic granitic intrusions;

- the western domain preserves a prograde Barrovian metamorphic sequence, ranging from slates, chlorite-muscovite schists in the west to staurolite, kyanite and sillimanite bearing schists in the east. These show, in places, scattered signs of partial melting close to the Joyeuse-Grimaud fault. Three main phases of deformation are identified. A first phase of ductile deformation (D1) is characterised by SE-directed thrusting, parallel to a strong stretching and mineral lineation in the western domain. In the eastern domain, ductile structures related to the D1 deformational phase are not preserved and it is assumed that they are entirely transposed by a deformation (D2) characterised by isoclinal and sheath folds, with a penetrative flat lying foliation S2. The S2 foliation bears a north-south trending L2 horizontal stretching and mineral lineation. Kinematic indicators suggest a top-to-the-south sense of shear. The phase D2 has evolved into orogen-parallel shearing along north-south trending, ductile dextral strike-slip shear zones (Ref). These zones of intense deformation are connected to the development of large-scale concentric folds and axial planar cleavage. During this transcurrent phase, two major faults (Joyeuse-Grimaud and La Moure faults) separated the massif into crustal-scale blocks with different exhumation histories [Morillon *et al.*, 2000; Corsini *et al.*, 2010]. The last phase of deformation (D3) is characterised by the growth of crustal anticlines and peraluminous granite (Plan-de-la-Tour – Rouet) and tonalite (Prignonet-Reverdit) intrusions. The Joyeuse-Grimaud and La Moure faults bound the eastern side of Carboniferous basins. Normal shearing-related fabrics are developed along limbs of crustal-scale antiforms and on the basins margins [Demoux *et al.*, 2008; Corsini *et al.*, 2010]. Therefore, the MTM exhibits during this late Variscan phase a

widespread extensional regime in the western part of the massif and E-W shortening, contemporaneous with strike-slip displacements along transcrustal faults in the eastern part.

2.2. Metamorphic and magmatic evolutions

The metamorphic evolution of the massif includes a HP-LT phase represented by eclogite relicts, largely overprinted by a MP-MT phase represented by Barrovian metamorphism in surrounding micaschists and migmatites, containing amphibolite lenses [Crevola *et al.*, 1994; Bellot, 2005]. Geochronological investigations in the MTM suggest that the high-pressure metamorphism occurred at ca. 430 Ma (U-Pb zircon in eclogite [Moussavou, 1998]; U-Pb monazite in orthogneiss [Demoux *et al.*, 2008]), which is also in agreement with HP-subduction related metamorphism ages in the French Massif Central [Matte, 2001]. The metamorphic evolution of the MTM, related to the Variscan collisional event, is started by MP-MT Barrovian regional metamorphism that developed during the nappe-piling process and which occurred between 350 and 330 Ma (U-Pb monazite in migmatitic orthogneiss [Demoux *et al.*, 2008]; U-Pb zircon on intrusives [Moussavou, 1998]). This event is followed by LP-HT regional metamorphism associated with the growth of migmatitic domes in the eastern part of the MTM and ductile normal faulting in the western part. As in most of the Variscan belt, the uplift of lower-crustal levels is ascribed to thermal relaxation and reequilibration of isostatic potential following crustal thickening [Faure, 1995; Ledru *et al.*, 2001].

However, the most specific tectonometamorphic phenomenon observed here is the vertical and passive amplification of antiforms typical of diapiric growth of the migmatitic lower crust, which always occurs in the general context of east-west shortening [Corsini *et al.*, 2009; Rolland *et al.*, 2009]. Heat and magma transfer were amplified by crustal scale shear zones, the Joyeuse-Grimaud and La Moure faults, that are believed to have controlled the late metamorphic evolution. The shearing must have been transpressive and highly partitioned, as the high-grade dome structures are found along the fault trend, in association with synconvergent tonalitic magmatism. This late event is dated by $^{40}\text{Ar}/^{39}\text{Ar}$ cooling ages on amphiboles, biotites and muscovites [Buscaill, 2000; Morillon *et al.*, 2000; Corsini *et al.*, 2010], which highlight the presence of three crustal blocks and indicate a distinct cooling history from 330 to 300 Ma. The western dip of the S1 foliation and the distribution of metamorphic isograds in the western unit are ascribed to an overall tilting of the uppermiddle crust during D2 [Rolland *et al.*, 2010]. This is corroborated by contemporaneous exhumation of the orogenic lower crust in the adjacent eastern unit, where several magmatic events have been rec-

ognized. An early magmatic event is characterized by the emplacement of anatectic granitoids around 340 Ma [Moussavou, 1998] corresponding to crustal melting during the thickening stage. This event is replaced by an incipient anatectic melting and emplacement of leucogranites at 320 to 315 Ma, related to an active tectonic exhumation and subsequent isothermal decompression following a phase of crustal thickening [Demoux *et al.*, 2008; Corsini *et al.*, 2010]. Finally syn- to late-kinematic granites, such as the Plan-de-la-Tour (Maures massif) and the Rouet (Tanneron massif) granites, are related to a dextral strike-slip shear zone at ca. 300 Ma. This later stage is contemporaneous with the deposition of Stephanian detrital sediments.

This massive augengneiss shows regular layering defined by high-grade mylonitic foliation. Ductile deformation is also marked by a strong horizontal stretching lineation and numerous shear criteria. Centimeter to meter-scale folds deform mylonitic foliation with vertical axial plane and horizontal axes parallel to the stretching lineation.

Migmatization is evidenced by coarse-grained granite-type leucosomes, which occur preferentially around K-feldspar megacrysts. Lenses of granitic melt that are taking place in asymmetric pressure shadows around feldspar indicates synkinematic anatexis. The orthogneiss is crosscut at high angle by several leucogranite dykes, which present either pegmatitic or aplitic textures. The co-existence of folds and horizontal shearing is indicative of transpressional context.

From geochronological point of view, the orthogneiss gives an age of 314 ± 2 Ma on muscovite and 308 ± 2 Ma on biotite obtained by $^{40}\text{Ar}/^{39}\text{Ar}$ method on single grain [Corsini *et al.*, 2010]. Leucogranite dykes cross-cutting the orthogneiss yields an age of 310 ± 2 Ma by $^{40}\text{Ar}/^{39}\text{Ar}$ [Corsini *et al.*, in prep.] and ages scattered between 295 and 320 Ma performed by ID-TIMS U/Pb on monazite [Demoux *et al.*, 2008]). These ages are interpreted as cooling of the HT metamorphism and subsequent melting of the orthogneiss occurring during exhumation in a regional transpressive context.

Stop 1.2 Cap Pinet metabasites:

Cap Pinet is located in the Eastern unit of the MTM, at the northern end of Pampelone Beach near St. Tropez. In this area the main lithologic units are migmatitic paragneisses associated to aluminous leucogranite dykes. Main foliation is sub-vertical with nearly N-S direction and bears a sub-horizontal stretching lineation. Unambiguous criteria allow defining a sinistral sense of shear with a top to the south displacement. Sheath folds parallel to stretching lineation and en echelon tension gashes perpendicular to stretching lineation which are filled with magmatic product argues for a transpressional regime synchronous of partial melting. Among these migmatites, two distinct basic bodies can be observed: (i) a 20 m wide N-S elongated lens of amphibolites made of numerous small sub-lenses; (ii) 0.5-1 m diameters rounded rigid boudins of garnet-rich metabasites, with serpentinite at the edge.

Deformation in the amphibolite lens is similar to surrounding migmatites. Basal section of the sub-lenses reveals a better preserved core relative to the strong stretching deformation recorded at the rim. The core shows granulite facies mineral assemblage (garnet, diopside, hypersthene, biotite, brown amphibole, plagioclase, ilmenite and quartz). The texture suggests retromorphoses from a previous eclogite (Kelyphite and symplectite), but no relictual omphacite has

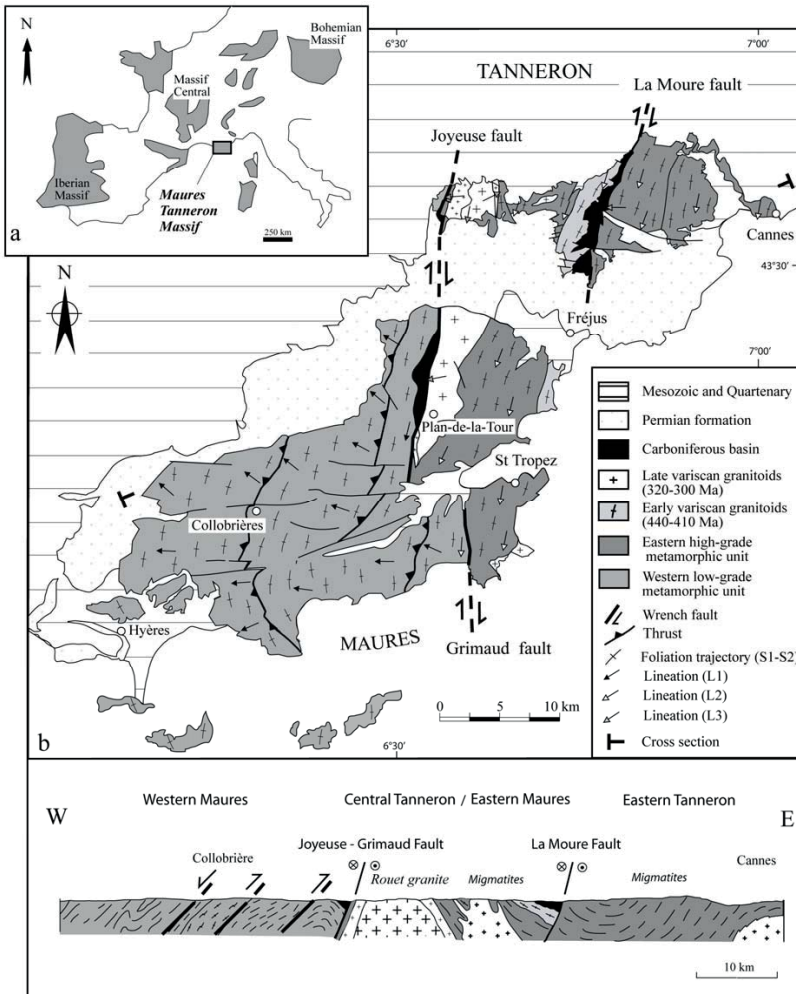


Fig. 1-1.- a: distribution of Pre-mesozoic units in Europe; b: simplified geological map and cross-section of the Maures-Tanneron massif (MTM), modified from [Corsini *et al.*, 2009].

Stop 1.1 Cannes - La Bocca orthogneiss:

Located at the easternmost part of the Maures-Tanneron massif (Fig. 1), this outcrop consists of migmatitic orthogneiss. The Cannes - La Bocca orthogneiss is a migmatitic augengneiss with very large K-feldspars megacrysts within a groundmass of quartz, perthitic K-feldspar, albite, biotite and muscovite which underlines the foliation. Large phenoblast of K-feldspar attest of the porphyric type of the granite protolith.

been found. The rim of the lenses show synkinematic reequilibration in amphibolite facies (pyroxene is replaced by green amphibole, minerals are all transposed in the lineation and relictual garnet is surrounded by plagioclase-amphibole pressure shadows). Geochemical analyses (major and trace elements) show N-MORB like signature for the protolith of the metabasites (Schneider *et al.*, in prep.).

The rigid boudins show foliation indicated by garnet-rich layers oblique to foliation of the surrounding migmatites. The boudins are garnet and diopside rich (granulite facies). Some calcite-rich veins transposed in the main foliation are observed. At the rim of the boudins, the granulite facies paragenesis is strongly reequilibrated in the amphibolite facies with diopside and garnet replaced by amphibole and plagioclase. Locally, greenschist facies paragenesis (epidote, chlorite, K-feldspar and sericite) replaces amphibole. The serpentinite shows relic minerals of a spinel-peridotite. Olivine is replaced by serpentine, enstatite by tremolite and spinel by Fe-chromite. Geochemical analyses revealed that those metabasites derived from the same protolith than the previous one but undergo two stages of hydrothermal alteration: (1) rodingitization prior the metamorphic imprint; (2) late metamorphic hydrothermalism in the greenschist facies.

$^{40}\text{Ar}/^{39}\text{Ar}$ dating on muscovites from the aluminous leucogranite dykes yield plateau ages of 300 ± 2 Ma. This age dates cooling of the unit during tranpressive exhumation.

Stop 1.3 La Croix-Valmer leptyno-amphibolic complexes:

This unit consists of a layered formation of amphibolite (meta-tholeiites with oceanic affinities; Seyler, 1986), pink orthogneiss (metamorphosed alkaline lavas; Seyler, 1986), and amphibole-biotite orthogneiss. It is interpreted as bimodal magmatism related to an extensional setting (Seyler, 1986; Briand *et al.*, 2002). The layered formation includes small lenses of meta-igneous rocks as parts of a supra-subduction zone lithosphere (Bellot *et al.*, 2000). A first group of abundant spinel peridotites, garnet-spinel peridotites, coronitic gabbros, garnet amphibolites, felsic amphibolites and fine-grained amphibolites was interpreted as portions of lithosphere generated in a supra-subduction zone during Early Palaeozoic time (Bellot, 2010). A second group of gabbros and fine-grained amphibolites was interpreted as portions of an oceanic lithosphere generated at the Cambrian-Ordovician boundary. Only garnet spinel peridotites are evidenced for HP metamorphism.

Zircon U-Pb dating on alkaline orthogneiss defines a Cambrian age for bimodal magmatism (498 ± 17 Ma and 507 ± 5 Ma; Lancelot *et al.*, unpub; $548 \pm 15/-7$ Ma; Innocent *et al.*, 2003). $^{40}\text{Ar}/^{39}\text{Ar}$ dating on amphibolites suggest cooling around 320 Ma of the central Maures in relation with its exhumation during the Namurian (Morillon *et al.*, 2000).

This unit exhibit isoclinal fold reworked by a strain-slip foliation, axial-plane of eastwards overturned folds, carrying a N110°E to N130°E striking stretching lineation. Thus, the stacking of these units may be considered as the result of southeastwards thrusting.

This unit is interpreted here as relics of a Cambrian (550-500 Ma) back-arc lithosphere involved in the Silurian continental subduction and the Carboniferous continental collision.

Stop 1.4 Canadel micaschists:

The outcrop consists of paragneiss, aluminous micaschist and quartzites. The metamorphic mineralogy is characterized by the association of quartz + feldspar + muscovite + kyanite + garnet + staurolite \pm andalusite typical of barrovian metamorphic sequence.

The NE-SW trending foliation is moderately dipping to the NW and bears a N trending mineral and stretching lineation. Asymmetric microstructures (S-C structures, shear bands) argue for a non-coaxial deformation with a top-to-the-NW normal shearing.

The micaschists give an age of 320 ± 2 Ma on muscovite obtained by $^{40}\text{Ar}/^{39}\text{Ar}$ method on single grain [Buscail, 2000]. This late orogenic extensional phase correspond to the collapse of the western domain of the MTM (Morillon *et al.*, 2000; Buscail, 2000; Bellot *et al.*, 2002).

The extensional tectonics of the western MTM follows a previous compressional event with nappe stacking where thrusting is synchronous with the regional MT-MP metamorphism. The contact at the base of the nappes is marked by a mylonitic zone with a top to the SE displacement (Bellot *et al.*, 2000; Bellot *et al.*, 2002).

References

- J. Bellot, The Palaeozoic evolution of the Maures massif (France) and its potential correlation with other areas of the Variscan belt: a review, in: R. Carosi, R. Dias, D. Iacopini, G. Rosenbaum (Eds.), The southern Variscan belt, J. Virtual Explorer, Electron., 19, 2005.
- F. Buscail, Contribution à la compréhension du problème géologique et géodynamique du massif des Maures : le métamorphisme régional modélisé dans le système KFMASH : analyse paragenétique, chémiographie, thermobarométrie, géochronologie $^{40}\text{Ar}/^{39}\text{Ar}$, PhD thesis, University of Montpellier, France, 2000.
- M. Corsini, Y. Rolland, Late evolution of the southern European Variscan belt: Exhumation of the lower crust in a context of oblique convergence, 341, 214-223, 2009.
- M. Corsini, V. Bosse, G. Féraud, A. Demoux, G. Crevola, Exhumation processes during post-collisional stage in the Variscan belt revealed by detailed $^{40}\text{Ar}/^{39}\text{Ar}$ study (Tanneron massif, SE France), *Int. J. Earth Sci (Geol. Rundsch.)* 96 1-9, 2010.
- G. Crevola, J.P. Pupin, Crystalline province: structure and Variscan evolution, in : J.D. Keppie (Ed.), Pre-Mesozoic geology in France and related areas, Springer Verlag, Berlin Heidelberg, 426-441, 1994.
- A. Demoux, U. Schärer, M. Corsini, Variscan evolution of the Tanneron massif, SE-France, examined through U-Pb monazite ages, *J. Geol. Soc.*, 165, 2008, 467-478.
- M. Faure, Late orogenic Carboniferous extensions in the Variscan French Massif Central, *Tectonics* 14, 132-153, 1995.
- P. Ledru, G. Courrioux, C. Dallain, J.M. Lardeaux, J.M. Montel, O. Vanderhaeghe, G. Vitel, The Velay dome (French Massif Central): melt generation and granite emplacement during orogenic evolution, *Tectonophysics* 342, 207-237, 2001.

P. Matte, The Variscan collage and orogeny (480-290 Ma) and the tectonic definition of the Armorica microplate: a review, *Terra Nova* 13, 117-121, 2001.

A.C. Morillon, G. Féraud, M. Sosson, G. Ruffet, G. Crévola, G. Lerouge, Diachronous cooling on both side of a major strike-slip fault in the Variscan Maures massif (SE France), as deduced from a detailed $^{40}\text{Ar}/^{39}\text{Ar}$ study, *Tectonophysics* 321, 103-126, 2000.

M. Moussavou, Contribution à l'histoire thermo-tectonique Varisque du Massif des Maures, par la typologie du zircon et la géochronologie U/Pb sur minéraux accessoires, thesis, University of Montpellier, France, 1998. Y. Rolland, M. Corsini, Metamorphic and structural evolution of the Maures-Tanneron massif (SE Variscan chain): evidence of doming along the transpressional margin, *Bull. Soc. geol. France*, special paper, 180, 3, 217-230, 2010.

The Variscan Corsica – Day 2 and 3 (May 20-21)

Philippe Rossi and Michel Faure

1. Geological setting

Corsica and Sardinia in the Variscan belt

The Maures Massif, Corsica and Sardinia (and southward Calabria and Kabylie) are a part of the “Southern Variscan realm” (SVR) that extends from Bohemia southward through the Alps (Fig. 2-1).

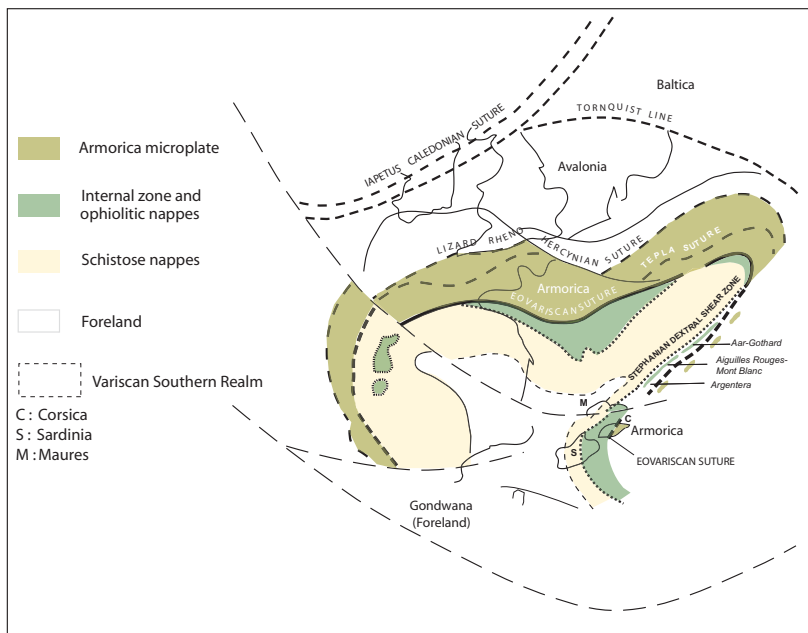


Fig. 2-1.- The southern Variscan realm in Western Europe. Permian Variscan zonation after Matte (2011).

Blocks within the SVR display many common characteristics such as the association of low-grade Panafrican and Eovariscan metamorphic basements and the presence of Mg-K granites. The present organization of the “SVR” can be considered to have resulted from the Stephanian drift, over hundreds of kilometres away from Eastern Bohemia (Rossi *et al.*, 2008), of dilacerated blocks along a transpressive dextral mega-shear zone as the result of the large clockwise rotation–translation of Gondwana towards North America (Bard,

1997). Palaeomagnetic measurements (Edel *et al.*, 1981) show that the Late Carboniferous Corsica-Sardinia batholith intruded a mosaic of exotic blocks; and that the Tethyan oceanization resulted in a partial dispersion/disappearance of Variscan chain. The final pattern was subsequently modified

by Alpine collision and the opening of Mediterranean back-arc basins. The Corsica-Sardinia microcontinent (CSM) was formed after a 30° Miocene anticlockwise rotation away from Europe. The CSM recorded two main magmatic events that sealed the respective position of host formations; the first at 340 Ma (prior to the major Stephanian dismemberment of the ‘SVR’), and the second between 330 and 280 Ma that have been used as ‘milestones’ in discussing the present and the palaeo-organization of the CSM.

A north-south transect of the CSM from the northern (Galeria) External Zone of Corsica to the southern (Iglesiente-Sulcis) External Zone of Sardinia (Fig. 2.2) shows in detail the general organization and lithological composition of the Internal Zone and the Nappe Zone (Carmignani *et al.*, 2001). The relation between the CSM and the Maures Massif is well explained by the original position of both Massifs before the Miocene rotation of the CSM. The palinspastic restoration reveals a close fits between Maures and

northwestern Sardinia that are documented by similar collision-related prograde tectonic-metamorphic features, post-collision evolution in the Variscan basement, as well as by strong similarities in the Mesozoic covers, including a Mid-Cretaceous bauxite-bearing stratigraphic interval (Mammeli *et al.*, 2007, Corsini *et al.*, 2009).

The structural frame of the CSM along studied transect is best exposed in Sardinia where the structural pile originated

Fig. 2-2.- Schematic section through the Variscan southern realm along the Corsica-Sardinia transects.

Legend - SU = Sulcis; FA = Flumendosa antiform; BS = Barbagia synform; BA = Barbagia antiform; MGMC = Medium grade metamorphic Complex; PAL = Posada-Asinara line; HGMC = High Grade Metamorphic Complex; Mg-K = Visean Mg-K plutonic rocks; g = Late Carboniferous - Early Permian batholith.

through a complex polyphase deformation (Carnignani *et al.*, 1979) that is characterized by a compressional event (D1) followed by a late extensional event (D2). The D1 event can be divided into three main syn-metamorphic phases: the first one generated south-verging overturned folds and top-to-south thrusts; the second is characterized by E-W shortening with top-to-west tectonic transport and exhibits a strong non-coaxial component and the third corresponds to a post-nappe piling folding resulting in broad upright antiforms and synforms consistent with a N-S shortening. The D2 event was characterized by a vertical shortening responsible for recumbent folding of previously steep fabrics, reworking of an older S1 foliation, and ductile to brittle low-angle normal shearing. The D2 phase ended with the emplacement of late-orogenic granite and the formation of Late Carboniferous to Early Permian basins that are common features in the South European Variscides.

In conclusion, a complete section of the southern realm of the Variscan orogenic belt can be restored in the Corsica-Sardinia segment. Northern Corsica exposes a nonmetamorphosed Palaeozoic succession lying on Panafrican mica schist related to a microcontinent (most likely Armorica or from a microcontinent from the Hun superterrane) that had drifted away directly from Gondwana. These formations are thrust over the Variscan Internal Zone composed mainly of anatectic high-grade Palaeozoic formations that crop out from central Corsica to northern Sardinia; the metamorphic peak of the eclogite remnants has been dated at c. 420 Ma. The Variscan Internal Zone interpreted here as a collision zone, and also the Eovariscan suture, was intruded in Corsica by Mg-K granite from 345 to 335 Ma. The thrust of this Internal Zone onto the stack of parautochthonous nappes in central Sardinia is cross-

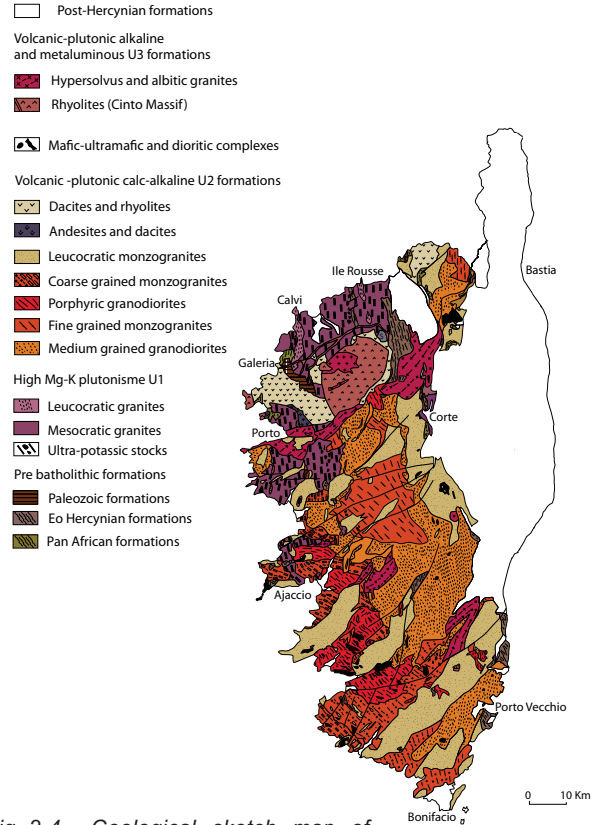


Fig. 2-4.- Geological sketch map of Corsica.

In Corsica, the Corsica-Sardinia batholith is constituted by:

- 1- "Magnesian-potassic" intrusions (U1) emplaced between 340 and 330 Ma. They are composed of quartzmonzonites and monzogranites and contain stocks and enclaves of comagmatic, ultra-potassic mafic rocks. The U1 intrusions are only exposed in western and northwestern Corsica, between Ile Rousse in the north and Ajaccio in the south.
- 2- "Calc-alkaline" plutonic intrusions and volcanites (U2) emplaced between 305 and 290 Ma form the main part of the batholith. The rocks are lighter in colour and include amphibole-biotite tonalgranodiorite to granodiorite, biotite-monzogranite and leucomonzogranite. The basic rocks associated with U2 magmas have a tholeiitic character and derive from a mantle magmatism that also gave rise to andesitic volcanic rocks and layered mafic-ultramafic complexes.
- 3- Alkaline volcanic and plutonic rocks (U3) emplaced at about 290 Ma. These U3 rocks, which are exceptional in Europe, are exposed in calderas eroded at different levels, from plutonic roots to volcanic formations.

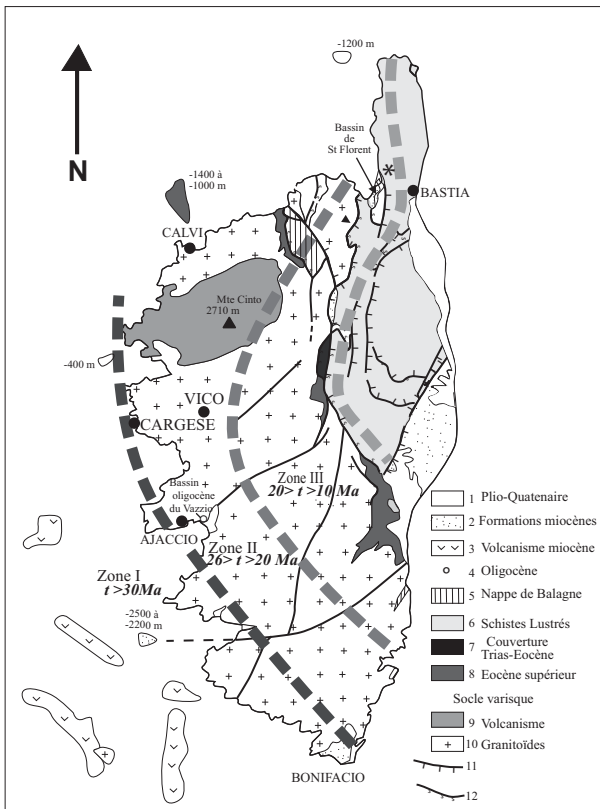
All the rocks of the batholith are cut by a network of acid and basic dykes that is fairly dense in places.

Fig. 2-3.- Geographic zoning of apatite FT ages in Corsica (Jakni *et al.*, 2000).

1: Plio-Quaternary, 2: Miocene, 3: Miocene calcalkaline volcanism (20-16 Ma), 4: Oligocene, 5: Alpine upper units, 6: 'Schistes Lustrés', 7: Triassic to Eocene cover, 8: Late Eocene, 9: Variscan volcanism, 10: granitoids.

Sharp landscapes constitute the most typical feature of Corsica, with a mean altitude of 568 m and its highest summit, Monte Cintu, culminating at 2710 m. Four other summits are higher than 2000 m (Monte Rotondo, 2622 m; Monte d'Oro, 2389 m; Monte Renoso, 2352 m; Monte Incudine, 2128 m). Apatite fission track (AFT) ages and measurements of track length distributions constrain its Cenozoic thermal and morphological evolution. AFT ages vary from 10.5±0.8 Ma to 53.8 ± 4.1 Ma and form a clear spatial pattern (Fig. 2-3): oldest ages are encountered in the SW of the island, with a broad band of ages between 20 and 30 Ma running across the mountainous central area and ages <20 Ma confined to the eastern half of the island. Samples along the W and NW coasts record km-scale erosional denudation linked to rifting in the Ligurian-Provençal Basin, whereas samples from close to the extensionally inverted Alpine deformation front record a later cooling phase related to Tyrrhenian extension. The eastward-younging pattern of AFT ages suggests the migration of a 'wave' of erosional denudation from west to east across the island, apparently controlled by the migrating locus of extension (Zarki-Jakni *et al.*, 2004).

The island of Corsica "A mountain in the sea"



cut by the Posada Asinara dextral shear zone. To the south, parautochthonous nappes overthrust the North-Gondwana margin which displays a possible Panafrican basement topped by an Iglesias-Sulcis nonmetamorphic/anchimeta-morphic Palaeozoic succession.

The Western Corsica (Fig. 2.4) is a part of the Corsica-Sardinia batholith. It consists mainly of Variscan granitoids and mafic complexes with local remnants of older metamorphic rocks that escaped erosion and represent the only relics of the batholith envelope.

Day 2: Sunday 20 May: En route from Bastia to Saint-Florent via the Alpine Corsica

The Alpine "Schistes lustrés" formation is a thick accumulation of nappes made up of ophiolites and marine deposits and enclosing fragments of continental basement derived from the Variscan batholith and its cover.

Finally, towards the very top of the nappe pile lies a synform of tectonic-sedimentary klippen involving paleomargin formations cropping out in the Nebbio nappe whose basal contact is masked to the north by the Saint-Florent Miocene formations.

During the Middle-Late Eocene the subducted HP-LT metamorphic formations were exhumed, and all the formations of the accretionary wedge were obducted westwards onto the Corsica craton. From Late Miocene (Tortonian, 11 Ma), all the accretionary wedge formations became emerged.

Stop 2-0 - Panoramic view from the Serra di Pigno summit (Fig. 2-5)

- In the distance the Variscan Tenda calc-alkaline volcanic-plutonic massif and its country rock (Agriate region). The massif, which acts as an Autochthon, at least relatively, suffered an Alpine ductile deformation in the greenschist facies. The finite strain here is heterogeneous and has resulted in almost unde-

formed to lightly deformed domains, bounded by ductile shear zones which developed at the same time as the schistosity.

- The Tenda massif and its sedimentary cover are thrust by the ophiolite bearing "Schistes Lustrés" nappe. The nappe is made up of polymetamorphic and polydeformed metasedimentary rocks of Late Jurassic-Cretaceous age, with Jurassic ophiolitic rocks, fragments of crust formed at the mid-ocean ridge, and slices of Variscan basement. In place, the "Schistes Lustrés" have been subjected to HP /LT metamorphism during the Alpine orogeny.

- Tectonically superimposed to the "Schistes Lustrés"nappe, the Nebbio depression occupies the centre of a synform made up of the structurally highest nappes, unaffected by Alpine metamorphism.

- Both the "Schistes Lustrés" and the Nebbio nappes are unconformably overlain by the Saint-Florent Miocene deposits.

- In the foreground, the Pigno unit is a Variscan granitic-gabbroic sliver inherited from the Tethyan Jurassic passive margin of Corsica and tectonically incorporated in the "Schistes Lustrés" nappe. The Pigno and associated alpine tectonic units are characterized by a lawsonite blueschist-facies metamorphism. They are made of Alpine metaophiolites and Variscan metagranitic and metagabbroic rocks with associ-

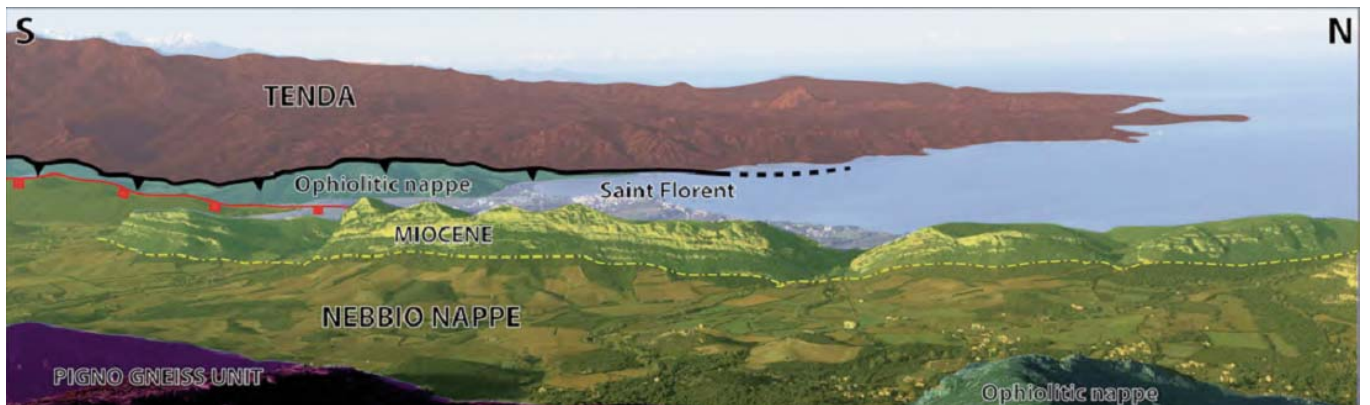


Fig. 2-5.- Panorama to the West from the Toghime pass. From Saint-Florent through the Agriate.

ated metasediments. PT estimated conditions are about 0.6-0.8 GPa and $300 \pm 50^\circ\text{C}$ in the Pigno unit and 1.0 GPa and 350°C in the Campitello unit (Lahondère, 1996).

From Saint-Florent through the Agriate.

Stop 2-1: Bocca a u Vezzo (Agriate), relationships between U2 Permian volcanic-sedimentary formations and leucomonzogranites

In the immediate eastern surroundings of the Bocca a Vezzu pass and on the southwestern part of the Monti Rossi sheets of fine-grained leucomonzogranite, half-meter thick, intrude volcanics of dacitic to rhyodacitic composition of the volcanic-sedimentary sequence.

In the northwestern part of the Tenda massif, the relationship between volcanism and plutonism can be sometimes difficult to observe because of Alpine reworking. The intrusion of

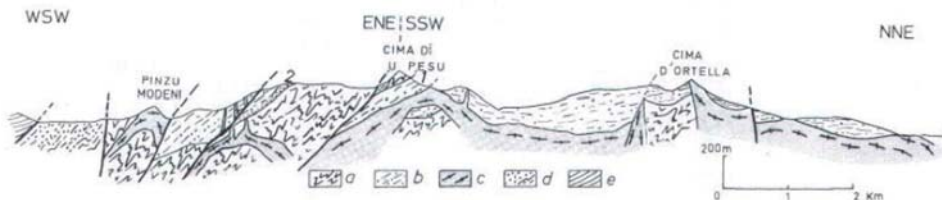


Fig. 2-6.- Synthetic interpretative cross-section (N-S) in the surrounding of Bocca a u Vezzo.

a: Panafrican metamorphic basement; b: volcanic sedimentary formations (VSF); c: leucomonzogranites; d: Autochthonous Eocene; e: Allochthonous of the Balagne nappe.

leucomonzogranites in the volcanic-sedimentary formations (VSF) may however be recognized in various places and namely immediately to the E of the Bocca a Vezzo (Rossi *et al.*, 1994). One can observe the intrusive contacts of granitic veins cutting VSF thanks to locally less intense Alpine deformation (Fig. 2-6). The intrusions of granites within the VSF developed a thermal metamorphism marked by the development of blastic biotites.

Rhyodacites of the upper part of the volcanic sequence were dated at 292.5 ± 2.2 Ma. The 281 ± 7 Ma age for the leucomonzogranite fits with field observations.

Stop 2-2: The Chierchiu panafrican basement and U2 "Chierchiu" upper-Carboniferous volcanic-sedimentary formation

The Panafrican basement is made of polydeformed micaschists, a latter pre-Hercynian deformation (Fig. 2-7). The unit is stabilized under greenschist-facies metamorphism, and no higher-grade relics have been found.

The composition of the metasedimentary rocks is intermediate between those of metaquartzite and metagreywacke, with varying amounts of ferrotitanium oxides. Residual sedimentary textures are common, with clearly identifiable S0 surfaces and S1 surfaces that resulted from a cleavage that roughly followed axial fold planes. Folds are outlined by phyllitic beds with muscovite, chlorite and sericite.



Fig. 2-7.- Panafrican micaschists are reworked by N-S decimetric zig-zag folds, reworking both the previous foliation and quartz exudates.

Within the sericite-chlorite micaschist, quartzitic beds alternate with phyllitic beds that commonly are clearly ribbon banded.

The metasedimentary formations (with interbedded amphibolite) are strongly refolded in certain areas (axial fold planes are oriented NNW-SSE) and characterized by the presence of centimetre-size almond-shaped quartz eyes that may fill up to about a quarter of the rock volume. Most of these exudations lie parallel to the foliation and their presence

outlines centimetre- to decimetre-size isoclinal folds, with rounded and thickened hinges and stretched limbs. Such areas with very high concentrations of quartz eyes are characteristic of shear zones that were intersected by U1 granite, which makes them older than 340 Ma.

Geochronological analysis of inherited zircon populations in micaschist sampled along the road between Chierchiu and the Bocca a Vezzu, provided an average age of 2081 ± 11 Ma (SIMS U-Pb zircon dating; Li, unpub. data).

Amphibolite is found in continuous levels, in places ribbon banded, up to several tens of metres thick and alternating with metasedimentary layers. The amphibolite shows a network of plagioclase that was transformed into albite and cryptozoisite; sulphides, ilmenite and ferrotitanium minerals are abundant. Deformation is outlined by syn-foliation amphiboles of a tremolite-actinolite composition that were created by the destabilization of pre-existing ferromagnesian minerals. Relict textures of ferrogabbro can be identified. Based on their chemical composition, these amphibolites can be considered as having been derived from enriched MORB-type basalt that may indicate an intracontinental-rift-type environment.

The Nd model age of the amphibolites falls around 600 Ma. A total-rock/minerals (ilmenite and amphibole) isochron gave an age of 747 ± 120 Ma for amphibolites sampled in the Cima a Forca Unit at Agriates (Rossi *et al.*, 1994). Although poorly defined, this measurement dates this metabasalt as between Late Proterozoic and Cambrian.

In the Argentella region (not visited), detrital Paleozoic rocks unconformably overlie the micaschist and amphibolite basement. They consist of conglomerates and Late Ordovician to Ashgillian shale. The shales are overlain by Late Ordovician (?) glaciomarine diamictites that are topped by graptolite-bearing Llandoveryan lydite (Barca *et al.*, 1996).

The Panafrican micaschist topped by nonmetamorphosed Palaeozoic succession were related to a microcontinent -most likely Armorica- and considered as the hinterland (Fig. 2.2) of the SVR (Rossi *et al.*, 2009).

Within the Chierchiu unit, it is possible to observe a U2 volcanic- sedimentary formation resting on the metamorphic panafrican basement. At the base of the VS formation is a monogenic conglomerate reworking the Panafrican basement (Fig. 2.8). The Chierchiu unit is a Upper Stephanian to Lower Permian volcano-sedimentary sequence that includes conglomeratic lenses.



Fig. 2-8.- Monogenic conglomerate lying on the Panafrican formations at the basis of the Chierchiu Upper-Carboniferous Volcanic-sedimentary Formation.

The Mg-K association

Stop 2-3: the Mg-K U1 association, Pula Pietra: vaugnerites and Santa Reparata quartzmonzonites

- A large body of “vaugnerite” (hosted into Monticello K-rich granodiorites) is visible on the shore. It is characterized by the abundance of K feldspar (41 vol. %), as poikilitic megacrysts, and biotite (25 vol. %); it contains in addition 4 vol. % Ca-rich clinopyroxene, 17 vol. % plagioclase and 4 vol. % accessory minerals (mainly titanite and apatite).

- Large blocks of Santa Reparata quartzmonzonites are visible on the way to the “vaugnerite” body. Santa Reparata quartzmonzonites are characterized by the abundance of K-feldspar megacrysts (up to 46 vol. %), mafic minerals (biotite, amphibole and residual clinopyroxene) and titanite, as “giant” crystals up to 1 cm long. Note the strong magmatic foliation and the flattened comagmatic enclaves.

The Eo-Variscan metamorphic formations

The metamorphic basement of Belgodere outcrops as a N-S trending ribbon, long 30 km for a width not exceeding 7 km (Palagi *et al.*, 1985). It is a disymmetric migmatitic dome displaying panels and enclaves of graywackes and sandstones locally preserved from melting along its western edge. These relics of the previous sedimentary formations were folded during an older phase prior to migmatization.

The metamorphic basement of Belgodere is composed of NS trending formations, from West to East: migmatitic gneiss and augen orthogneiss, migmatite, “leptynic-amphibolic” (LA) formations, micaschist, quartzite and migmatitic gneiss and leucogranite. LA is composed of the association, at every scale, of leptynite, sometimes augen, gneiss, quartzite, amphibolitic gneiss and amphibolite. All these formations suffered a strong and polyphased synmetamorphic deformation that completely transposed all previous markers.

In the least deformed rocks, magmatic textural relics can still be observed revealing the cumulative gabbroic origin of some amphibolite.

Recrystallization is polyphased as attested by many reactions and mineral zonation.

The following successive parageneses can be distinguished in metabasic rocks: 1) garnet + zoisite + rutile + brown hornblende; 2) green and blue-green hornblende + plagioclase (andesine-oligoclase) + clinzoisite + titanite + pistacite + quartz; 3) actinolite + plagioclase + chlorite + calcite + titanite + pistacite + sericite + quartz. Moreover magnetite, ilmenite, apatite, zircon and sulphides are present.

The oldest metamorphic parageneses (without plagioclase), in equilibrium with garnet, would represent an early eclogitic stage. Phenoclastic garnet is rounded by a secondary symplectite of plagioclase-amphibole-epidote. On the other hand, the rutile is also unstable and rimmed by titanite. Finally the existence of former pyroxene is suggested by the poikiloblastic habitus of amphiboles.

The “leptynites” leucocratic augen- (or not) gneiss are composed of quartz, plagioclase, orthoclase, biotite or muscovite. Garnet and sillimanite are often present as relics suggesting the existence of a stage of very high pressure and high temperature (eclogite and granulite facies).

The quartzites are very fine grained (recrystallized quartz) and often contain muscovite and chlorite.

The crystallization of stilpnomelane, pumpellyite, and phengite in a large part of the rocks of the Belgodere metamorphic complex is the result of an Alpine reworking.

Stop 2-4: Relationships between the U1-Mg-K plutonism and the Hercynian metamorphic basement of Belgodere

Outcrop, point 323 on the road RD 11 (from Belgodere to Occhiatana). Both side of the bridge.

"Orthogneiss" are intercalated within the mainly metasedimentary "Gneiss of Belgodere" formation (Laporte and Orsini in Rossi *et al.*, 2000). Geologic mapping reveals that these "orthogneiss" are km scale folded (NNE-SSW axis) but the ductile deformation of the orthogneiss is weak (no foliation, rectangular shaped feldspars etc.).

As these "orthogneiss" contains biotite, amphibole and clinopyroxène and microgranular enclaves, they can be considered as Mg-K intrusions.

Geometric relationships between "orthogneiss" and the migmatitic Gneiss of Belgodere (from East to West or from Belgodere to Occhiatana) can be observed through different outcrops along the D11 road:

- a metric layer of "orthogneiss" is intercalated (sub) conformably within the migmatitic layered gneiss. The "orthogneiss" is clearly distinct and in contact with anatectic leucosomes (frequently "en boudins") within the dark micaeous gneiss. No foliation does appear in "orthogneiss": the K-spars are globally oriented parallel to the contacts. Both "orthogneiss" and migmatitic gneiss are intersected by late leucocrates veins (outcrop in the quarry).

- The "orthogneiss" includes a metric enclave of migmatitic gneiss. The "orthogneiss" display varying textures (more or less porphyric and macro crystals of variable size). The orientation of macro crystals is roughly parallel to the foliation the gneiss; the other contacts between enclave and matrix are locally diffuse. Similar observations can also be realized on blocks along the road or used for construction the sheepfold.

To the E of the bridge, "orthogneiss" are dominant and display enclaves of varied composition: ± micaeous gneiss, amphibolite, migmatite.

The synkinematic character of the "orthogneiss" is obvious: it is a Mg-K granitic rock which intruded contemporary to late to anatectic phenomena. "Orthogneiss" was dated at 338.1 ± 0.1 (U-Pb on zircon, Paquette *et al.*, 2003). This chronology is in agreement with observations realized at regional scale *i.e.* absence of thermal contact between Mg-K granites and basement.

The road to the eastern part of the metamorphic complex at Belgodere goes through the Asco Canyon and crosscuts the hypersolvus granites of the Popolasca Complex (Fig. 2-9).

Stop 2-5 The P3 unit of the Popolasca complex

The composition of the pink hypersolvus granite is: perthitic K-feldspar, albite and euhedral rounded quartz. The Fe-rich biotite has a late crystallization and is almost always chloritized. Thorite is as common as zircon but thorite-zircon (mixed grains) are frequent but, whatever their habitus, both minerals are metamict. Allanite and more rarely the cassiterite can be identified, late fluorite is common.

The REE patterns of granites of the 3 units of the Popolasca complex are shown on figure 2-10. From P1 to P3 one can observe the transition from highly fractionated REE patterns, with a weak negative Eu anomaly in the P1 mesocratic granite, to REE patterns where the Eu negative anomaly is deeper in P2 in conjunction with an increase of the

The U3 A-type Popolasca complex

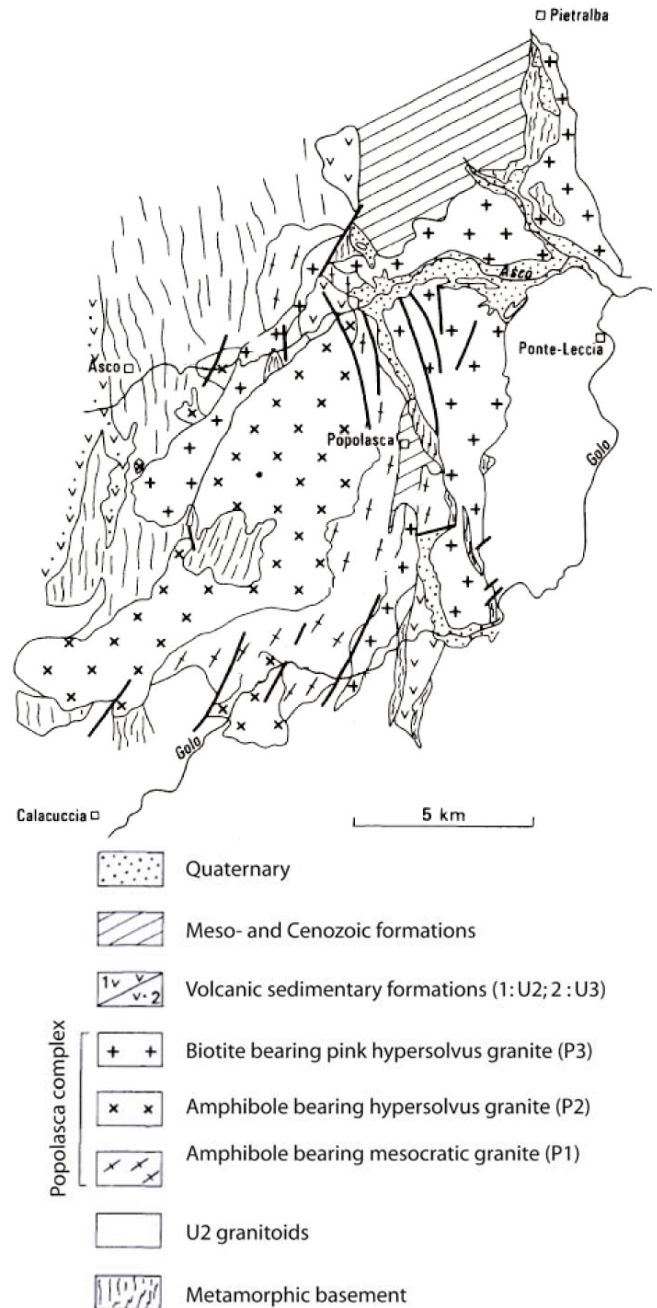


Fig. 2-9.- Sketch map of the U3 Popolasca plutonic complex.

The metaluminous A-type Popolasca complex (Rossi *et al.*, 1994), exposed over some 30 km², is composed of three successive concentric, crescent-shaped hypersolvus-granite units: P1, amphibole bearing mesocratic granite; P2, amphibole bearing hypersolvus granite and P3, biotite bearing hypersolvus pink granite. A U-Pb age was measured on the P1 external unit of amphibole mesocratic granite. The rock contains amphibole (ferro-magnesian hornblende) and rare relics of clinopyroxene and biotite [0.73 < X_{Fe} < 0.85] commonly occur as aggregates with associated allanite. Quartz is automorphic and occurs in grouped crystals. Most of the feldspars are perthitic K-feldspar, but some oligoclase crystals are present and rimmed by albite. Zircon grains are transparent, large (up to 0.3 mm) and abundant. Three methods used to date on zircon (Pb-Pb evaporation, TIMS and SHRIMP) provided exactly the same age within their respective analytical errors (Cocherie *et al.*, 2005). An average weighted age of the three results can be calculated at 290.2 ± 1.8 Ma (Cocherie *et al.*, 2005).

HREE. In the P3 unit, the REE fractionation is very low: the pink granite is characterized by a flat pattern and a very deep negative Eu anomaly. The REE patterns of previous U2 "calc-alkaline" can be roughly compared to the U3 granites of the

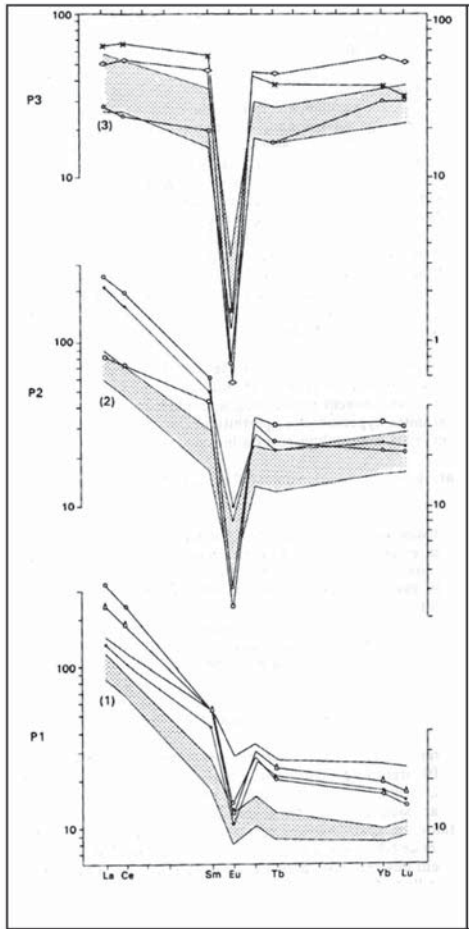


Fig. 2-10.- REE patterns of the 3 units (P1, P2 and P3) of the U3 plutonic complex of Popolasca. The grey areas represent the envelope of the REE patterns of U2 granodiorites (1), monzogranites (2) and leucomonzogranites (3).

Popolasca complex; they show similar REE distributions but at significantly lower levels. The similarity between the behavior of the REE (and other trace elements) in the U3 Popolasca complex and in U2 calc-alkaline granitoids, suggests that the magma evolution was controlled by the same processes in the two associations (a mechanism of fractional crystallization). Isotope values of Sr ($Sr_i = 0.708$ on Popolasca granites) and oxygen ($7.7 < \delta^{18}O_{\text{‰}} < 9.8$, extreme values for units P1, P2, P3) display continental crustal characteristics and are comparable to those of the U2 calc-alkaline granitoids.

Stop 2-6: The Belgodere metamorphic complex in the Asco Canyon

At the contact with the Belgodere metamorphic complex, the Popolasca granite (P3) displays a fined grained margin (locally chilled or pegmatitic).

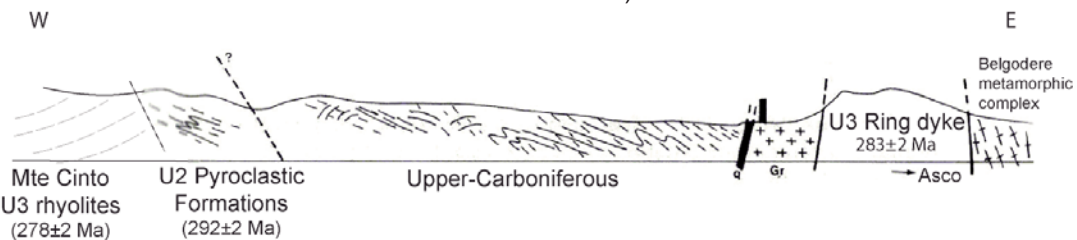


Fig. 2-12.- (from Durand Delga et al., 1977) E-W section on the edge of the Monte-Cinto Lower Permian caldera.



Fig. 2-11.- Migmatitic gneiss (West of the Asco Canyon)

Migmatitic gneiss outcrop immediately to the East of the contact, (Fig. 2-11) they are composed of quartz, plagioclase, K-feldspar, biotite or muscovite ± sillimanite. They probably rework a volcanic sedimentary formation. The protolith was respectively dated (U-Pb SHRIMP on zircon) at 476 ± 8 Ma (Rossi *et al.*, 2009) for fine grained gneiss and at 478 ± 7 Ma for augengneiss (Lower Ordovician). These rocks can be compared to the Iberian “Ollo de Sapo” or Armorican “Porphyroïdes” formations dated between 490 and 470 Ma. Moreover, they contain Neoproterozoic inherited zircons dated at 624 ± 10 Ma indicating they were derived, for a large part, from the melting of Cadomian material. Older inherited ages were obtained at 1 Ga and 2.07 Ga.

The peak of metamorphism and anatexis was dated at 337 ± 8 Ma on monazite (EPMA). This result fits with field data showing that there is no thermal contrast with the U1 Mg-K rocks emplaced at c.a 345-330 Ma.

Stop 2-7: the Cauldron subsidence of Monte Cinto

This section is situated on the edge of the Eastern part of the Monte Cinto caldera.

One can observe from E to W: i) the gneiss of the metamorphic complex of Belgodere ~in contact (fault) with a large microgranitic (50 m) U3 ring dyke dated at 283 ± 2 Ma; ii) U2 granites crosscut by rhyolitic dykes on some meters and Upper Carboniferous dark schistosed pélites [these pelites where dated in the Mausoleo basin (paleoflora) at 5 km to the North], iii) schistosed Lower Permian U2 pyroclastic formation (292 ± 2 Ma) thrust by the Upper Carboniferous formation; iv) fault at the external limit of the cauldron and U3 rhyolites (278 ± 2 Ma) and pyroclastites (U-Pb/zr ages, unpublished).

Day 3: Monday 21 May, from Corte to Bonifacio

Stop 3-1: The granulitic paragneiss "kinzigites" of the Santa Lucia nappe basement

The outcrop displays a septum of granulitic paragneiss (banded "kinzigite") located 20 m from the contact with the SL mafic complex in the Campetiu River (altitude 300 m) west of Punta Falconaghja.



Fig. 3-1.- The banded kinzigites of the Santa Lucia nappe.

The paragneiss ("kinzigites", Fig. 3-1) is fine grained and locally contains centimetre-wide quartz-feldspar anatectic veinlets testifying to the presence of melts. It displays a primary mineral assemblage of pyrope-rich garnet, sillimanite, K-feldspar, biotite, both clear and pinkish zircon, rutile and spinel, for which peak P-T metamorphic conditions were calculated at $PGpa = 0.7 \pm 0.1/T^{\circ}C = 800$ (Libourel, 1985) or $PGpa = 1/T^{\circ}C = 900$ (Caby and Jacob, 2000).

The presence of plagioclase banding is interpreted as the result of strong partial melting in a granulitic environment. The "restitic" layers, 1-10 cm thick, comprise a quartz-depleted matrix with an assemblage of biotite-plagioclase-cordierite (destabilized) plus garnet as residual clasts. Libourel (1985) describes a progressive replacement of the primary K-feldspar-garnet-rutile assemblage ($PGpa = 0.7 \pm 0.1/T^{\circ}C = 800$) in the more common paragneiss by a lower P-T secondary association with cordierite-biotite-rutile ($PGpa = 0.45-0.6/T^{\circ}C = 750-800$).

Winged porphyroclasts and sigmoidal features reveal a constant pervasive shearing that took place under slightly decreasing P-T conditions, as testified by cordierite-biotite mineral assemblages. Similar deformation has been described from the Ivrea Zone (Brodie *et al.*, 1989) with concomitant extensional faulting.

U-Pb SHRIMP data on zircon from Santa Lucia (Rossi *et al.*, 2006) provided ages ranging from to 356 to 157 Ma (Fig. 3-2), with a major frequency peak at 285 Ma (with

exception of one inherited Archean grain). The zircons are considered to have been formed by metamorphic processes after burial in the lower crust.

To summarize, the granulitic metasediment from Santa Lucia reached lower-crust conditions no later than 400 Ma (Early Devonian). They remained within this high P-T environment until they were brought to the surface during Jurassic crustal thinning; ophiolites were dated between 169 Ma and 152 Ma (U-Pb/Zr on trondhjemites).

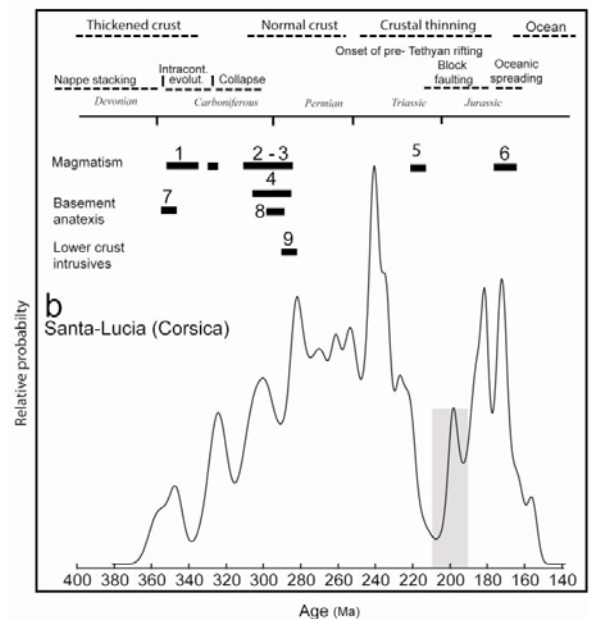


Fig. 3-2.- Relative probability plots of U-Pb zircon spot ages for the Santa Lucia granulitic metasediment vs. time-location graph of the main geological events in the upper-crust, including crustal thickening and thinning and the geodynamic environment. Grey box: Nd/Sm age of granulitic metasediment.

Broken line: crustal thickness; structural environment (see text). Thick lines: Upper crust magmatic and metamorphic events. 1: monzonitic magmatism; 2: calc-alkaline magmatism; 3: alkaline and/or metaluminous magmatism; 4: mafic tholeiitic magmatism; 5: Triassic volcanism - oceanic magmatism; 6: Jurassic ophiolite; 7-8: main anatectic episodes; 9: Santa Lucia mafic complex (from Rossi *et al.*, 2006).

The Variscan basement around Porto Vecchio

The Porto-Vecchio basement is exposed over some tens of kilometres from Solenzara-Fautea series in the North to the Chiappa series in the South, these formations were studied by G. Libourel (1985) and Giacomini *et al.* (2008).

- The Solenzara-Fautea series is mainly composed of garnet-kyanite granulitic paragneiss enclosing pyroxenite and pyrigarnite boudins, the southern and western parts being bounded by migmatite.

- The Chiappa series consists, from south to north, of porphyric orthogneiss, a leptynic-amphibolic complex, and fine-grained micaschist.

The Solenzara-Fautea series

Stop 3-2: Granulitic paragneiss: Sea shore Tarcu



Fig. 3-2. Close-up photo of the garnet bearing paragneiss on the Tarcu sea shore.

a. Primary assemblages

The garnet-kyanite granulitic paragneiss occurs as irregular bands of quartz-feldspar leucocratic layers, depleted in garnet, and darker layers of same composition but enriched in biotite and garnet. They are commonly spotted by muscovite and blue kyanite is easily visible.

Along the sea shore of Tarcu, granulitic paragneiss is remarkably conserved in the granulite succession as well as in migmatitic gneiss. Not showing any trace of retrograde metamorphism, these assemblages are composed of: quartz - garnet (alm-pyr) - perthitic K feldspar - antiperthitic plagioclase (An 20-25) - kyanite - rutile - zircon - apatite - graphite.

Textures are granoblastic to granolepidoblastic; globular or sub-automorphic garnet, commonly with helicitic inclusions, shows perfectly stable contacts with the K-feldspar. Kyanite, as elongated rods in the foliation plane or oblique to it, in places shows small inclusions of automorphic garnets, rutile, quartz and biotite. The stability of the garnet and the K-feldspar, as well as the presence of kyanite as the only aluminium silicate, indicate that the associations reflect a granulitic high-pressure episode.

b. Assemblages showing retrograde metamorphism

Retrograde metamorphic assemblages are marked by the development of biotite and muscovite associations at the expense of the initial garnet and K-feldspar assemblages, following a reaction of the type $Gt + FK + H_2O \leftrightarrow Bi + Mu + Qz$.

Garnet is enveloped by closely associated Bi + Mu over a limited distance. Occasionally, in granulite that underwent further retrograde metamorphism such as in the Conca stream near the migmatitic Fautea gneiss, this reaction results in garnet atolls that were drowned in a biotite and

muscovite felting. Secondary quartz progressively moulds the garnet shape, which tends to disappear.

In parallel to the development of these assemblages, kyanite is commonly surrounded by a muscovite halo with quartz droplets, at the contact with K-feldspar. Such destabilization is caused by a reaction of the type: $Ky + FK + H_2O \leftrightarrow Mu + Qz$. As before, various operating stages of this reaction can be observed. The kyanite disappears in the end, leaving a few quartz granules within the muscovite felt.

The later stages of retrograde metamorphism remain entirely within the kyanite stability field, as is suggested by the accidental appearance of sillimanite in this granulitic succession, as well as the direct pseudomorphism of kyanite into andalusite. Finally, the development of chlorite at the expense of garnet must be attributed to these same processes of retrograde metamorphism.

Stop 3-3: Mafic granulite: Ogliastriccione, seashore north of Tarcu

In the southern area, mafic granulite has been found in the Tarcu cove and 500 m north of on the shore. Dark green in outcrop, these extremely massive rocks contain garnet that can be recognized everywhere. In addition, these rocks are commonly loaded with amphiboles from the centre to the edges of the boudins or lenses. In certain cases, the lenses are surrounded by an amphibole "cortex", with or without garnet.

The primary paragenesis of these rocks is composed of clinopyroxene + garnet (alm-pyr, rich in grossular ~30%) + plagioclase (~An 50) + quartz (\pm) rutile and opaques. Notwithstanding a, locally strong, secondary amphibolitization, this paragenesis is characterized by the co-stability of garnet and clinopyroxene in the presence of plagioclase. These metabasic rocks thus define a high-pressure granulite (pyrigarnite), even though the eclogite s.s. domain has not been reached.

The first stages of the later amphibolitization of this paragenesis are shown by characteristic kelyphitic textures, witnessing of retrograde metamorphism under hydrating conditions. The extreme stages of this metamorphism led to a complete resorption of garnet; the pyrigarnite boudins thus changed into common amphibolite, as can be seen in the migmatites of Ogliastriccione, where swarms of boudins present different stages of retrograde metamorphism.

Estimation of P-T granulitic assemblages

The primary crystallization conditions of the granulitic assemblages were determined from the Gt - FK - Plag - Ky - Bi - Qz association in granulitic paragneiss that did not suffer retrograde metamorphism and the Cpx - Pl - Gt - Qz association in slightly amphibolitized pyrigarnite.

The different geothermobarometers used shows them to be relatively concordant, indicated that the primary parageneses were created under pressures between 1.2 and 1.5 GPa and temperatures between 800 and 900°C. These, rigorous, values that agree with the mineralogical assem-

blages, indicate that these rocks at one point in their history underwent high-pressure metamorphism.

Based on Vielzeuf's thermodynamic work (1980, 1984) on the stability fields of the Gt - Fk assemblage, one can assume that the Bi + Mu + Qz and Mu + Qz associations in the paragneiss that developed at the expense of Gt - FK and Ky + FK mark a high-pressure start of the retrograde metamorphism. The history of the subsequent retrograde metamorphism falls entirely within the kyanite stability field, as is attested by the absence of Ky + Sill pseudomorphs. This means that, based on the primary conditions, one cannot envisage a pressure decrease at constant temperature here.

Nevertheless, the presence of kyanite and andalusite pseudomorphs marking the end of this retrograde metamorphic evolution, as well as the partial re-equilibration of pyrigarnite in the amphibolite facies, indicate that the retrograde metamorphism was characterized by a major pressure decrease. Based on the stability conditions of the triple point of aluminium silicates, the formation of these last assemblages might effectively indicate a pressure difference of around 0.6-0.7 Gpa, when compared with the primary conditions.

Pyrigarnite geochronology (JYC 39)

The youngest age at 345.2 ± 4.7 Ma (10 points) was measured on large zircon rims. It corresponds to the age of the anatexis of the basement as constrained in other parts of the Variscan basement, such as Belgodere. The 560 ± 50 Ma and 688 ± 20 Ma ages are considered as inherited. Ages

pointing to 466 ± 30 Ma (4 points) are seen as the age of the protolith, whereas ages at 440 ± 12 Ma and 412 ± 32 Ma are interpreted as those of the metamorphic climax (Fig. 3-5).

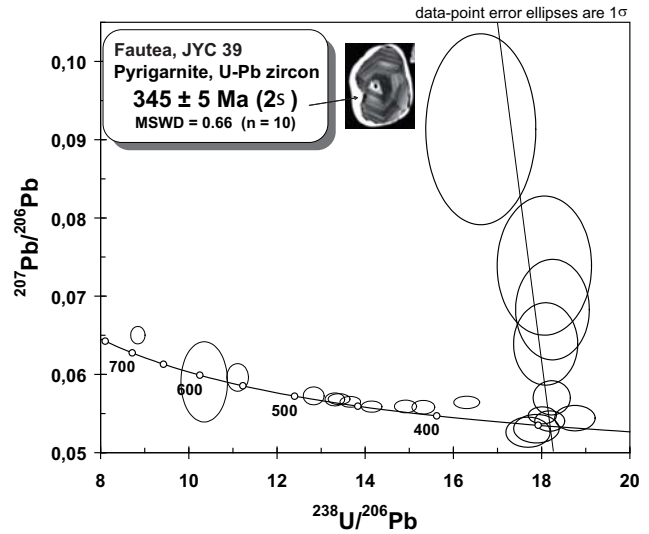


Fig. 3-5.- U-Pb/Zircon dating of the pyrigarnite from Fautea (Rossi et al., 2009).

A structural, petrological and geochronological (U-Th-Pb of zircon and monazite) study (Giacomini et al., 2008) proposes that the lower crust sequences of the Variscan high-grade basement cropping out between Solenzara and Porto Vecchio, have been tectonically juxtaposed along with middle crustal rocks during the extrusion of the orogenic root of the Variscan chain.

It is proposed that a system of high temperature, orogen-parallel shear zones that developed under a transpressive dextral tectonic regime caused the exhumation of the entire sequence. This tectonic complex is thus made up of rocks having undergone different P-T conditions (eclogite-? high-pressure granulite facies and amphibolite facies) at different times, reflecting the progressive foreland migration of the orogenic front.

The Solenzara granulites were derived from burial of continental crust to high-pressure (1.8-1.4 GPa) and high- to ultrahigh-temperature conditions (900-1.000°C) during the Variscan convergence: U-Pb ELA-ICPMS zircon dating constrained the timing of this metamorphism at c.a 360 Ma.

The **gneisses cropping out at Porto Vecchio** are middle crustal-level rocks that reached their peak temperature conditions (700–750°C at <1.0 GPa) at ca. 340 Ma. The diachronism of the metamorphic events, the foliation patterns and their geometry suggest that the granulites were exhumed to middle crustal levels through channel flow tectonics under continuous compression.

The amphibolite facies gneisses of Porto Vecchio and the granulites of Solenzara were accreted through the development of a major dextral mylonitic zone forming under amphibolite facies conditions: in situ monazite isotope dating (ELA-ICPMS) revealed that this deformation occurred at c.

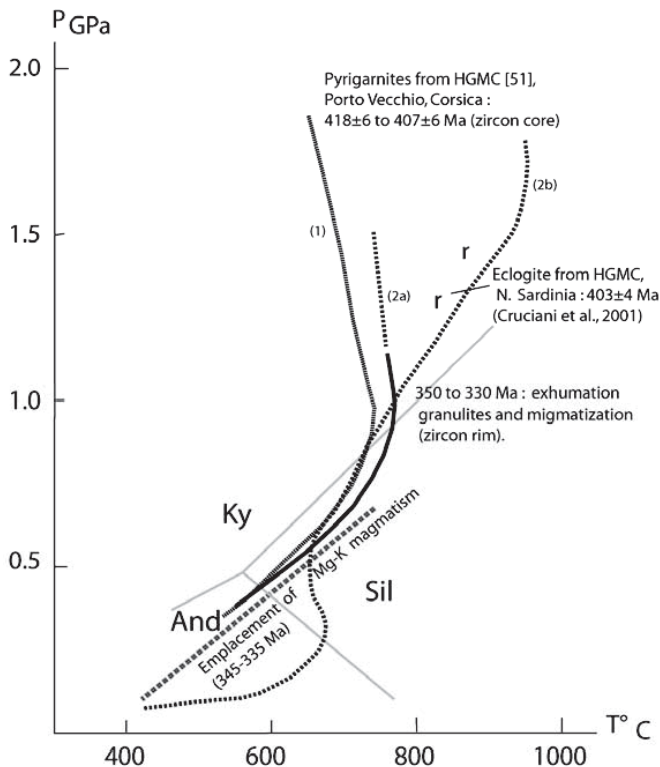


Fig 3-4.- P-T paths for HGMC rocks from Southern Corsica (1): Porto Vecchio, (after Giacomini et al., 2008) and Northern Sardinia (2a): metabasites (2b): gneiss, after (Giacomini et al., 2005, 2006).

320 Ma and was accompanied by the emplacement of syn-tectonic high-K melts.

A final HT-LP static overprint, constrained at 312-308 Ma by monazite U-Th-Pb isotope dating, is related to the emplacement of the igneous products of the Sardinia-Corsica batholith and marks the transition from the Variscan orogenic event to the Permian extension.

Stop 3-4: Leptynite-amphibolite complex: Punta di Fautea

At Fautea, we can see a fragment of the leptynite-amphibolite complex, previously described by Arthaud and Matte (1975) and Ricci and Sabatini (1978). The biotite amphibolite is ribbon banded, with a grano-nematogranoblastic texture. The compositional ribbons are marked by alternating amphibole- and plagioclase-rich levels. Biotite occurs as long lamellae that intersect the foliation and seem to post-date it. Pale-green amphibole, dominating many ribbons, is statistically elongated in the main foliation plane. Calcic (and-lab) plagioclase occurs as polygonal assemblages. No aluminium silicates were observed.

Between the Punta di Fautea and the Anse de Favone, granulitic rocks are only exposed in the southern sector over a distance of 6 km, between the Bocca di a Guardia in the north and the Conca stream in the south. They are mainly composed of alternating granulitic paragneiss layers in which are sporadic boudins or lenses of basic granulite, whose size can vary from around 10 cm to over 50 m. Occasional marble lenses occur near Cervonicchia, intercalated in these rocks, either as thin laminated layers, or as small centimetre-size boudins. This core of granulitic rock is surrounded by migmatitic gneiss, exposed in the north around Punta Telica and Tossa Rossa, and in the south near Fica and around Ogliastriccione and the Punta di Fautea.

Within these migmatitic zones, amphibolite boudins, with or without garnet, are commonly observed; granulitic levels persist sporadically in the migmatitic gneiss of Ogliastriccione (southern area).

In the southern sector, the general foliation of the succession oscillates between N010° et N030° with a steep easterly dip. To the south, around Fautea, the foliation gradually changes to a generally east-west direction with a steep northerly dip. Within the granulite, a syn-metamorphic lineation has a variable pitch of 40° to 80°N in the foliation plane.

The Chiappa series

Metamorphic formations of the Chiappa are N-S cropping out between the intrusion of the Varra leucomonzogranite at their roof and Eocene conglomerates of Piccovaggia that hide its eastern extension.

To the North, metamorphic formations are intruded by granodiorite of Porto-Vecchio. The contact, almost always hidden under the sea is observable at Punta di Chiappa. The follow-

ing succession can be observed from the south to the North: i) porphyric orthogneiss ; ii) leptynic-amphibolite and iii) fine paragneiss exposed namely at the foot of the hill of the lighthouse.

The general foliation draws a large bow with concavity towards the NW, foliation is oriented from N125 to N90 on the hill of the lighthouse, dip is subvertical.

Stop 3-5: The leptyno-amphibolite complex

It consists of repetitive vertical layers of leucocratic gneiss so called "leptynites" and amphibolites also associated with porphyric gneiss. The thickness of the complex does not exceed 800 m. It outcrops along the road down to Marina Vizza as well as on the coast to the East of Marina de Arje.



Fig. 3-6.- Photo of the leptynic-amphibolite complex on the sea shore East of Marina de Arje.

Stop 3-6: The Chiappa micaschists (from Libourel, 1985 and Giacomini *et al.*, 2008)

The "Chiappa micaschists" group a set of rocks where are associated quartz-feldspathic (\pm muscovite) layers alternating with biotite-muscovite- (\pm sillimanite and garnet) of fine grained gneiss and micaschists that suffered an intense rotational deformation. Rare kyanite relicts were found within plagioclase. They are both exposed on the hill of the lighthouse. Shear zones displaying intense mylonitic deformation contain clasts of garnet and plagioclase and clusters of white mica in which often persists andalusite relicts. In some samples, fine-grained biotite developed without preferred orientation over the pre-existing foliation and pinite aggregates around garnet relicts testify to the presence of former cordierite replacing garnet. Micaschist display association similar to those of the paragneiss; however garnet seems more abundant. Paragneiss and the fine grained gneiss are chloritized.

Stop 3-7: The porphyric orthogneiss

The porphyric orthogneiss found in the Chiappa area is quite widely exposed in the surrounding area. Specifically,

good outcrops occur 4 km to the southeast, on Forana Island (Cerbicale islands).

Its texture is that of a systematically porphyroclastic metagranite, generally with "eyes" of K-feldspar, 2 to 3 cm long but exceptionally as large as 5-10 cm, as well as of polygonal plagioclase that can enclose garnets. Biotite "1" and muscovite occur as spindles. A post-deformation, non-rotational, metamorphic episode is characterized by unoriented biotite "2". This metagranite has an aluminous composition, hosting uncoloured and clear zircons, locally as elongated prisms conferring them an acicular aspect; their average A-T index of 232-384 is characteristic of zircons from aluminous magmas.



Fig. 3-7. Photo of the Chiappa porphyroclastic augengneiss.

References

- Arthaud F., Matte P. (1977) - Détermination de la position initiale de la Corse et de la Sardaigne, à la fin de l'orogénèse hercynienne, grâce aux marqueurs géologiques anté-mésozoïques. *Bull. Soc. géol. Fr.*, (7), T.XIX, n°4, p. 833-840.
- Barca S., Durand-Delga M., Rossi Ph., Štorch P. (1996) - Les micaschistes panafricains de Corse et leur couverture paléozoïque: leur interprétation au sein de l'orogène varisque sud-européen. *C. R. Acad. Sci. Paris*, IIa, **322**, 981-989.
- Bard J.P. (1997) - Démembrement anté-mésozoïque de la chaîne varisque d'Europe occidentale et d'Afrique du Nord : rôle essentiel des grands décrochements transpressifs dextres accompagnant la rotation translation horaire de l'Afrique durant le Stéphanien. *C. R. Acad. Sci., Paris*, IIa, **324**, 693-704.
- Caby R., Jacob C. (2000) - La transition croûte-manteau dans la nappe de Santa-Lucia-di-Mercurio (Corse alpine) : les racines d'un rift permien. *Géologie de la France*, **1**, 21-34.
- Capelli B., Carmignani L., Castorina F., Di Pisa A., Oggiano G., Petrini R. (1992) - A Hercynian suture zone in Sardinia: geological and geochemical evidence. *Geodinamica Acta* **5**, 101-118.
- Carmignani L., Coccozza T., Minzoni N., Pertusati P.C., Ricci C.A. (1979) - E' la Corsica il retropaese della catena ercinica della Sardegna? *Mem. Soc. Geol. It.* **20**, 47-55.

The metagranite (Gneiss de Sotta PV97B) was dated at 463 ± 14 - 11 Ma (U-Pb TIMS zircon, Rossi *et al.*, 2009). On Forana Island, the dating of monazite in the metagranite gave an age of 338 ± 6 Ma, which corresponds to the passage of $T^\circ\text{C}$ below 690 ± 40 (Dahl, 1997) after the metamorphic peak.

Porphyric orthogneiss is common in the basement of the Corsica-Sardinia batholith. In the Zicavo series of Corsica, aluminous metagranite has been dated (Pb-Pb evaporation on zircon) at 458 ± 32 Ma and, by U-Pb on zircon, in Belgodere at 476 ± 8 Ma and in Sardinia at 456 ± 14 Ma in the Lodé aluminous metagranite (Helbing & Tiepolo, 2005).

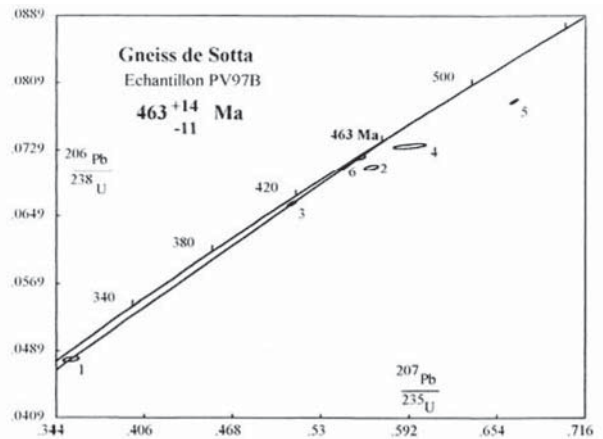


Fig. 3-8.- U-Pb –zircon dating of the porphyric orthogneiss from the Chiappa series.

- Carmignani L. (coord.), Oggiano G., Barca S., Conti P., Salvadori I., Eltrudis A., Funedda A., Pasci S. (2001) - Geologia della Sardegna. *Memorie descrittive della Carta geologica d'Italia*, v. IX, 283 p.
- Cocherie A., Albarède F. (2001) - An improved U-Th-Pb age calculation for electron microprobe dating of monazite. *Geochim. Cosmochim. Acta*, **65**, 4509-4522
- Corsini M., Rolland Y. (2009) - Late evolution of the southern European Variscan belt: Exhumation of the lower crust in a context of oblique convergence, **341**, 214-223.
- Dahl P.S. (1997) - A crystal-chemical basis for Pb retention and fission-track annealing systematics in U-bearing minerals, with implication for geochronology. *Earth Planet. Sci. Lett.*, **150**, 277- 290.
- Daniel J. M., Jolivet L., Goffé B., Poinssot C. (1996) - Crustal-scale strain partitioning: footwall deformation below the Oligocene-Miocene Alpine detachment of Corsica. *J. Struct. Geol.*, **18**, 41-59.
- Edel J.B., Montigny R., Thuizat R. (1981) - Late Paleozoic rotations of Corsica and Sardinia: new evidence from paleomagnetic and K-Ar studies. *Tectonophysics*, **79**, 201-223.
- Giacomini F., Dalla L., Carminati E., Tiepolo M., Ghezzi C. (2008) - Exhumation of a Variscan orogenic complex: insights into the composite granulitic-amphibolitic metamorphic basement of south-east Corsica (France). *J. Metamorphic Geol.*, **26**, 403-436.

- Guillot S., di Paola S., Ménot R. P., Ledru P., Spalla M.I., Gosso G., Schwartz S. (2008) - Two Variscan suture zones in the External Crystalline Massifs of Western Alps and the importance of the dextral ECMs shear zone for Palaeozoic reconstruction (submitted to Intern. J. Earth Sciences).
- Jakni B, Poupeau G., Sosson M., Rossi Ph., Ferrandini J., Guennoc P. (2000) - Dénudations cénozoïques en Corse : une analyse thermochronologique par traces de fission sur apatites. *C. R. Acad. Sci., Paris*, t. 324, série IIa, p. 775-782.
- Lahondère, D. (1996) - Les schistes bleus et les eclogites a lawsonite des unités continentales et océaniques de la Corse alpine; nouvelles données pétrologiques et structurales. Documents BRGM, 1996, vol. 240, 285 p.
- Libourel G. (1985) - Le complexe de Santa-Lucia-di-Mercurio (Corse). Ultramafites mantelliques, intrusion basique stratifiée, paragneiss granulitiques. Un équivalent possible des complexes de la zone d'Ivrée. Doctoral thesis, Université Paul-Sabatier, Toulouse, 461 p.
- Libourel G., Vielzeuf D. (1988) - Isobaric cooling at high pressure, example of Corsican granulites. *Terra Cognita*, **8**, p. 268.
- Helbing H., Tiepolo M. (2005). Age determination of Ordovician magmatism in NE Sardinia and its bearing on Variscan basement evolution. *Jour. Geol. Soc. London*, **162**, 689-700.
- Mameli P., Mongelli G., Oggiano G., Dinelli E. (2007) - Geological, geochemical and mineralogical features of some bauxite deposits from Nurra (Western Sardinia, Italy): insights on conditions of formation and parental affinity. *International Journal of Earth Sciences*, **96**, 877-902.
- Mameli P., Mongelli G., Oggiano G., Dinelli E. (2007) - Geological, geochemical and mineralogical features of some bauxite deposits from Nurra (Western Sardinia, Italy): insights on conditions of formation and parental affinity. *International Journal of Earth Sciences*, **96**, 877-902.
- Palagi P., Laporte D., Lardeaux J.M., Ménot R.P., Orsini J.-B. (1985) - Identification d'un complexe leptyno-amphibolique au sein des « gneiss de Belgodere » (Corse occidentale)., *C. R. Acad. Sci. Paris*, Ser. II 301, 1047-1052.
- Paquette J.-L., Ménot R.-P., Pin C., Orsini J.-B. (2003) - Episodic and short-lived granitic pulses in a post-collisional setting: evidence from precise U-Pb zircon dating through a crustal cross-section in Corsica. *Chemical Geology*, **198**, 1-20.
- Ricci C.A., Sabatini G. (1978) - Petrogenetic affinity and geodynamic significance of meta-basic rocks from Sardinia, Corsica and Provence. *N. Jb. Mineral., Mh.*, **1**, p. 23-28.
- Rossi Ph., Lahondère J.-C. Lluch D., Loÿe-Pilot M. D., Jacquet M. (1994) - Feuille Saint-Florent - Carte géologique France (1/50 000) - Orléans : BRGM. Notice explicative par Rossi Ph., Lahondère J.-C. Lluch D., Loÿe-Pilot M. D. et coll.
- Rossi Ph., Cocherie A. (1991) - Genesis of a Variscan batholith: field, mineralogical and geochemical evidence from the Corsica-Sardinia batholith. In: The European Geotraverse, Part 7. *Tectonophysics*, **195**, 319-346.
- Rossi Ph., Durand-Delga M., Caron J.M., Guieu G., Conchon O., Loÿe-Pilot, M.D., Rouire, J. (1994) - Geological Map of France at 1:50 000 scale, Corte Sheet (1110), BRGM Orléans.
- Explanatory Notes : Ph. Rossi, M. Durand-Delga J.M. Caron G. Guieu, G., O. Conchon, G. Libourel, M.D. Loÿe-Pilot (in French).

Sardinia – Days 6, 7 and 8 (May 24-26)

Giacomo Oggiano, Stefano Cuccuru, Antonio Funedda, Leonardo Casini

The Variscan Orogeny in Sardinia 1. General framework

The Sardinian part of the South Variscan Realm (SVR- Fig. 1a) shows an almost complete orogenic section, from the high-grade, mainly migmatitic, axial zone in the northern area (Fig. 1b) to the non-metamorphic fold-and-thrust belt foreland in the south western edge of the Island (Fig. 1b). A thick pile of allochthonous greenschist units are continuously exposed between the axial zone and the foreland (Fig. 1b). The allochthonous greenschist units record quite a complicate sequence of tectonic/metamorphic events, still poorly correlated with the evolution of the high-grade axial zone.

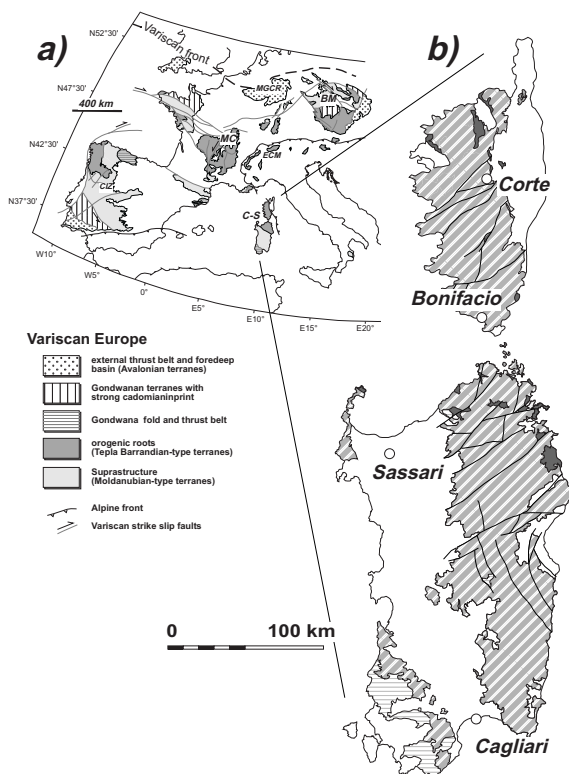


Fig. 1.- Sketch map of the Variscan basement of Europe (a) and the Corsica-Sardinia block (b).

The main shortening phase (D1 - Carmignani *et al.*, 1992; 1994; Gerrei and Meana Phases - Conti *et al.*, 2001) was responsible for piling of tectonic units. D1 is characterized by top-to-the S or SW direction of tectonic transport developing south-verging isoclinal folds and thrusts, well preserved in the greenschist zone and the foreland. In the axial zone, due to anatexis and superposition of later deformations, they are generally not recognizable in the field although occasionally con-

served within large orthogneiss or mafic bodies. The age of D1 is not precisely constrained, however some amphibole Ar/Ar age on sheared metabasites, together with Rb/Sr on muscovite from micaschists in northern Sardinia suggest that syntectonic assemblages have grown around 350 Ma. This age is roughly consistent with the inferred age of partial melting in migmatites from the NE Sardinia, yet constrained between 355 and 345 Ma by Rb/Sr on leucosomes (Ferrara *et al.*, 1978) and, more recently, by U/Pb on zircon (Giacomini *et al.*, 2006). The age of D1 is still poorly defined in the greenschist zone and the foreland, as no direct radiometric dating has been presented. In the southern part of the Island, however, fossiliferous upper Devonian-lower Carboniferous sequences are deformed and metamorphosed within south-directed D1 structures. There is no evidence for involvement of Visean strata (Conti *et al.*, 2001). From these records and lacking more precise geochronologic constraints, one can argue that D1 deformation was almost coeval in the axial zone and the more external sectors of the chain. Although this apparently positive match, the beginning of deformation in the axial zone should be placed some 10-20 Ma backward, taking into account the incubation time required for crustal thickening to create anatexis conditions as those recorded by the axial zone.

A second shortening phase D2 (Sarrabus Phase - Conti *et al.*, 2001) characterized by top-to-the W direction of tectonic transport caused stacking of the Sarrabus Unit (Fig. 2 from Conti *et al.*, 1999) onto the previous south-directed pile of tectonic units. Deformation is still associated to low-greenschist facies metamorphism and is supposed to be of lower Carboniferous age, that is, little younger than D1. The possible correlation of such event to shear zones and other D2 structures (Carmignani *et al.*, 1992; 1994) dated around 320 Ma (Di Vincenzo *et al.*, 2004; Carosi *et al.*, 2012) in the axial zone is still unresolved, because of lack of robust geochronological constraints in the greenschist units.

Finally, the last shortening (Flumendosa Phase - Conti *et al.*, 2001) produced km-scale open synforms and antiforms oriented from NW-SE to roughly W-E in the very southern part of the nappe stack (Fig. 2). These structures, presently still undated, developed under diagenetic or very low-grade metamorphism and are not associated to penetrative foliations.

A phase of post-collisional extension (Rio Grappa Phase - Conti *et al.*, 2001) characterized by vertical shortening led to thermal doming, development of metamorphic core-complexes (Conti *et al.*, 1999; Casini & Oggiano,

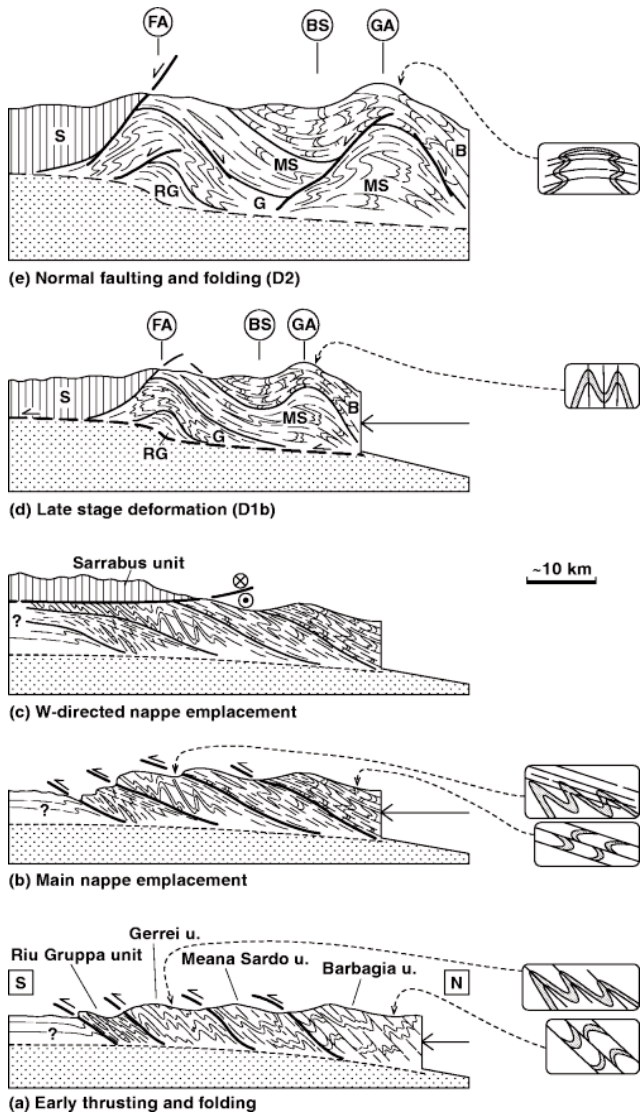


Fig. 2.- Main Variscan tectonic phases as recognized in the external Nappe zone (redrawn from Conti et al., 1999).

2. The high-grade zone

2.1. The HGMC

The Variscan crust in north Sardinia (Fig. 4 from Casini et al., 2012) is mainly represented by granitic massifs, closely associated to migmatitic complexes hosting subordinate, largely re-equilibrated, mafic bodies and orthogneisses that record HP-HT granulitic metamorphism (Giacomini et al., 2005; 2008; Cruciani et al., 2008). Anatectic bodies, migmatitic gneisses, orthogneisses and mafic bodies were collectively identified to as the High-Grade Metamorphic Complex (HGMC in Carmignani et al., 1994), that has been tentatively correlated to the Tepla Barrandian-type terranes of central Europe (Rossi et al., 2009). Following this model, the amphibolite-facies and lower grade metasediments (MGMC - Medium Grade Metamorphic Complex, Carmignani et al., 1994) have been interpreted as the remnants of the accretionary wedge that accumulated onto the northern passive margin

2008) and normal faulting. Several authors suppose that extension is grossly coeval with the construction of the Corsica-Sardinia Batholith (C-SB, Carmignani et al., 1992; 1994; Conti et al., 2001; Carosi et al., 2009), however recent structural analysis and U-Pb zircon ages from Sardinian granites challenged this view (Oggiano et al., 2005; Oggiano et al., 2007; Casini et al., 2012). New geochronologic constraints suggest in fact that early plutons started to grow around 320 Ma, that is, almost coeval with the strike-slip deformation recorded by ductile shear zones in the northern and central part of Sardinia (Di Vincenzo et al., 2004; Carosi et al., 2011). Besides, among several petrogenetic models (Rossi & Cocherie, 1991; Ferré & Leake, 2001), dissipation of viscous shear heating has been proposed as a key mechanism for generating the melts in the C-SB (Fig. 3 from Casini et al., 2012).

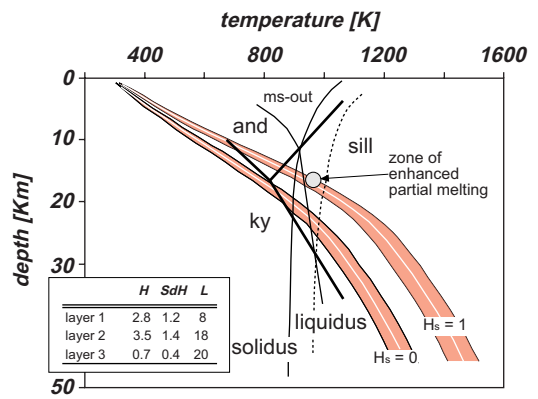


Fig. 3.- Simplified 1D thermal model of the Variscan crust: the higher-T geotherm involves a component of shear heating.

of Gondwana in Ordovician-Carboniferous times. This interpretation seems to be meaningful from several points of view. The HGMC is, indeed, a crystalline nappe which experienced HT-metamorphism and anatexis during exhumation, though at places small bodies of felsic HP-granulites and re-equilibrated eclogites have been identified (Giacomini et al., 2005). Because of extensive amphibolite-facies re-equilibration and discontinuous exposure amongst the granitic massifs, it is quite speculative to establish whether the HT-metamorphism is still related to crustal shortening rather to post-collisional extension, however most interpretations point to an overall extensional setting which should have favored thermal relaxation and partial melting, with positive feedbacks on extension (Giacomini et al., 2005; 2006; Cruciani et al., 2008; Casini et al., 2012). Recent U-Pb dating on zircon rims suggests that partial melting in the HGMC possibly began at around 345 Ma, as indicated by the age of

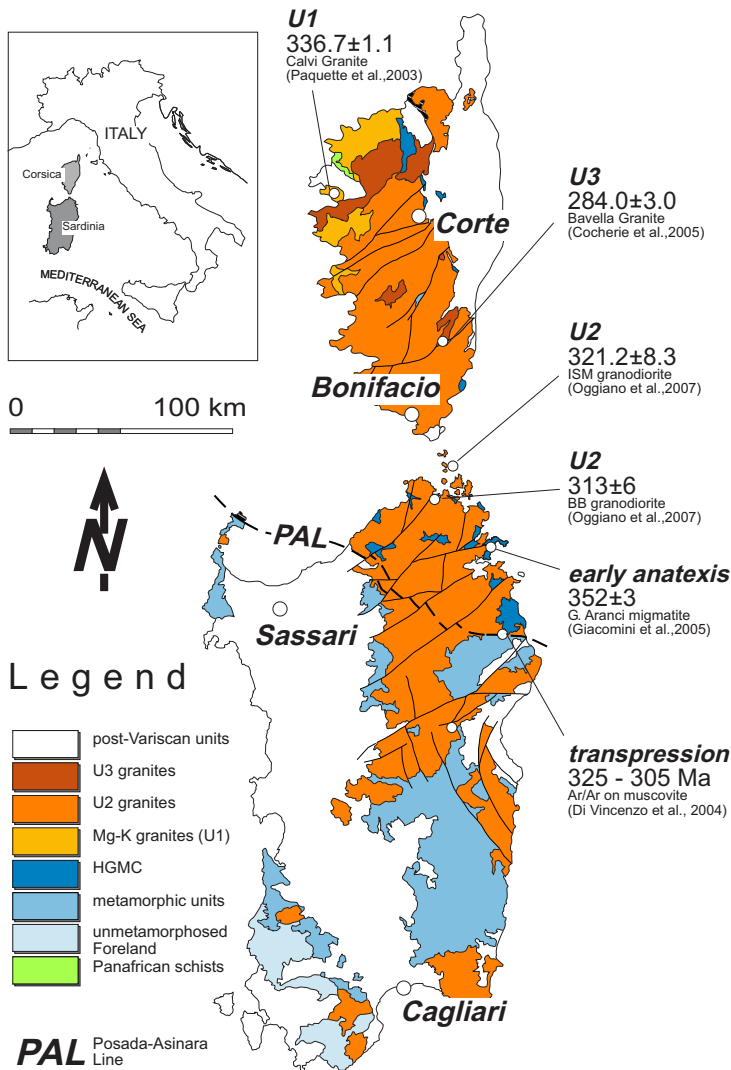


Fig. 4.- Structural sketch map of the Corsica-Sardinia block.

migmatitic gneisses in the Golfo Aranci area (Giacomini *et al.*, 2005; 2006). Anatexis of the Variscan crust is a major event in the Corsica-Sardinia block from about 350-345 Ma (Ferrara *et al.*, 1978; Giacomini *et al.*, 2006). The early melts consist of trondhjemitic leucosomes that reflect focused anatexis of metasediments by muscovite dehydration melting (Cruciani *et al.*, 2008b). Somewhat younger leucosomes characterized by granodioritic and granitic composition testify higher solidus temperatures and increased rates of melting of an heterogeneous crust (Cruciani *et al.*, 2008a; Macera *et al.*, 2011).

2.2. The Posada-Asinara Line

The Posada-Asinara Line (PAL, Fig. 4 - Carmignani *et al.*, 1992; 1994) is a major tectonic lineament that separates the migmatitic massifs to the north and the amphibolite-facies metasediments, to the south. This structure is a D2 steep NW-SE ductile, dextral shear zone (2-4 km thickness) reactivated under low greenschist-facies conditions. Recently, a more complex tectonic history has been proposed. Carosi *et al.* (2011) suggest, in fact, that early activity along the PAL was accommodated by top-to-NW displacement; then (320-300 Ma - Carosi *et al.*, 2011), the

kinematic suddenly switched to dextral, generating the observable structure. Relicts of this early motion would be preserved within rigid fragments that survived later deformation. According to Casini *et al.* (2010) instead, the PAL originated as a ductile thrust with top-to-the SW transport direction, then deformation switched to one of dextral transpression; evidence for early reverse motion along the PAL are

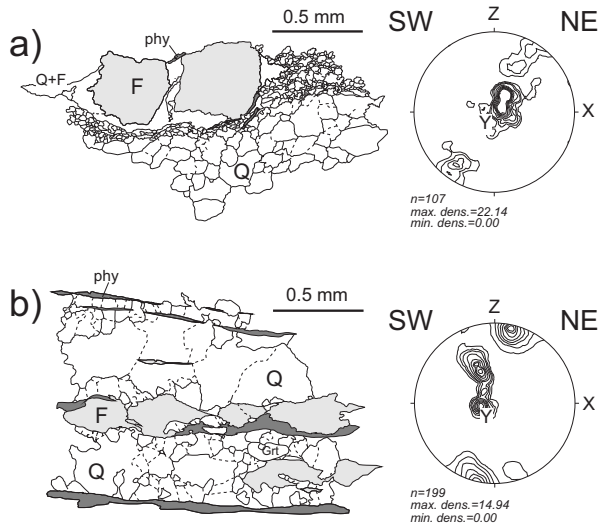


Fig. 5.- Quartz-feldspar microstructure and quartz c-axis fabric within mylonite in the PAL (sample location close to Giuncana).

nically preserved by quartz texture in dynamically recrystallized quartz + muscovite + kyanite veins (Fig. 5).

It is worth noting that poorly deformed boudins of grt-amphibolites with relicts of eclogitic mineral assemblages have been identified within the high-strain zone of the PAL (the phyllonitic zone), close to the village of Giuncana.

In the early 1990's, Capelli *et al.* (1992) evidenced that the protholiths of metabasites with relic eclogitic assemblages (Fig. 6) found along the PAL have a N-MORB type affinity. This geochemical composition was explained in terms of subduction of an inferred pre-Cambrian oceanic crust. Recent U-Pb ages found on magmatic zircon cores constrain instead the protholith age in the lower Ordovician; an early Devonian (c.a. 400-410 Ma) age for the HP-event is suggested on the basis of U-Pb ages obtained from different metabasite bodies (Pta de li Tulchi - Palmeri *et al.*, 2004; Giuncana - Cortesogno *et al.*, 2004). The short time span between the crystallization of protholiths and subduction (< 40-50 Ma), altogether with the relatively high temperatures recorded during the HP event (T > 600-620°C for P < 1.8-2.0 GPa) indicates that subduction was not one of "Alpine-type". Two possible explanations could be: i) the mafic bodies scattered along the PAL derive from short-lived subduction of a small back-arc basin that opened in middle Ordovician and closed in early Devonian; ii) the PAL does not represents a suture zone, rather it is a sort of regional-scale back thrust through which part of the South-Armorican Ocean was

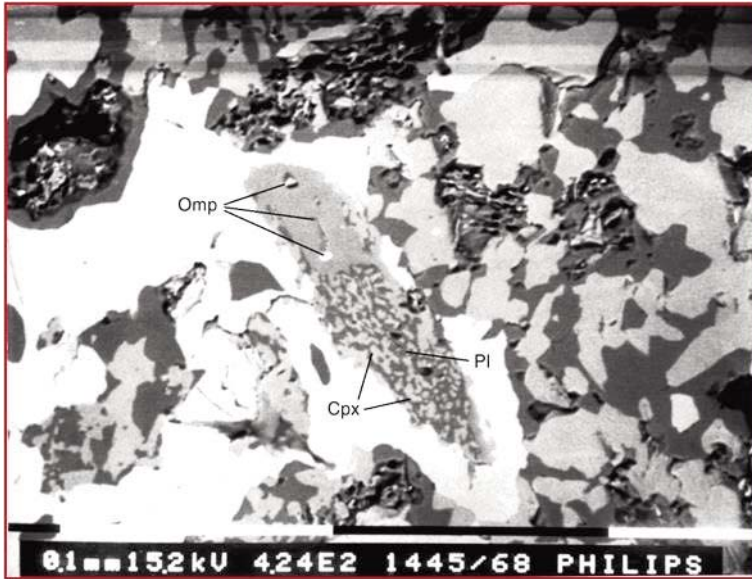


Fig. 6.- Clinopyroxene-plagioclase corona around former omphacite (*Giuncana eclogite*).

channeled toward Gondwana during continuous south-directed subduction. In this model, back thrusting pathways are controlled by the geometry of previously extended regions along the northern Gondwana margin,

as incipient rifting might have caused softening and heating of the crust.

2.3. The MGMC

The MGMC metapelites display garnet + biotite + oligoclase and kyanite + garnet + staurolite assemblages that indicate quite a typical Barrowian-type evolution. The age of metamorphism in the MGMC is constrained between 355-335 Ma from Ar/Ar on syntectonic biotite, amphibole and muscovite and suggest, therefore, that peak metamorphic conditions in the MGMC were approximately coeval with anatexis in the overlying HGMC. This metamorphic stage has been correlated with the early phase of crustal shortening, characterized by a top-to-the S-SW direction of tectonic transport (D1 phase of Carmignani *et al.*, 1994). Giving these evidences, it seems reasonable that both complexes might have experienced a radically different tectonic and metamorphic evolution. Actually, the recognized strike-slip character of the PAL suggests that the HGMC could have been translated toward SE (in present-day coordinates) by tens to hundreds of km, relative to the inferred stable north Gondwana margin represented by the MGMC.

3. The nappes and foreland

3.1. The greenschist nappe pile

The metamorphic basement of central and south Sardinia consists of a thick pile of greenschist facies tectonic units showing sedimentary/volcanic sequences that range in age from the lower Cambrian to the early Carboniferous. The more internal unit is the monotonous Barbagia Unit, whereas the more external Meana Sardo, Gerrei, Riu Gruppa and Sarrabus Units show a larger compositional heterogeneity (Fig. 34).

All these units share a common lithostratigraphic sequence characterized by minor differences in the Ordovician volcanic-sedimentary level and different thickness of the lower Carboniferous Pala Manna flysch (Fig. 35). Three main angular unconformities subdivide the palaeozoic succession into four sedimentary cycles. The oldest unconformity separates the Cambrian-lower Ordovician from the overlying volcanic complex referred to as middle-upper Ordovician. This unconformity is known since the first half of the 20th century as 'Discordanza Sarrabese' (Calvino, 1959b), which was correlated by the same author to the 'Sardic Phase' established by Stille (1939) in the Iglesias area. The second discordance is a non-conformity separating the shallower part of the Ordovician volcanic complex from the upper Ordovician sedimentary succession (Caradocian Transgression Auct.). Somewhere along the non-conformity, parts of the volcanic arc are completely missing because of depositional hiatus, or focused erosion.

The third of these unconformities separates the siliciclastic and carbonatic succession of Silurian-lower Carboniferous

age from the lower Carboniferous clastic sediments, occasionally interpreted as the product of sin-orogenic erosion of the orogenic wedge (Barca, 1991; Barca *et al.*, 1992; Maxia, 1983). The four unconformity-bounded sedimentary sequences can be recognized, with minor differences, throughout the whole Nappe zone (Fig. 35): the base of Cambrian sequences start with meta-sandstones, phyllites and conglomerates collectively known as the S. Vito fm (Calvino, 1959b). Palaeo-depositional reconstructions indicate that sediments were accumulated within shallow submarine fan-delta, near shore face or intertidal environments. It is worth noting that the base of the Nappe zone succession lacks any record of Cambrian carbonates, which are indeed exposed in the more external fold and thrust belt zone (SW Sardinia). This difference suggests that a stable passive margin - possibly coincident with the northern margin of Gondwana - was maintained only in the very SW part of Sardinia till the lower Ordovician. The contact separating the S. Vito fm from the overlying lower-middle Ordovician succession is discordant and often marked by meta-conglomerates (Muravera Metaconglomerates fm, Carmignani *et al.*, 2001b). The Ordovician sequence consists of a magmatic complex composed of meta-volcanic rocks and meta-sedimentary rocks derived from early reworking of volcanic materials (epiclastite). The composition of volcanic rocks vary from the one of basalt to rhyolite, with abundant meta-volcaniclastic rocks and meta-conglomerates. This association is collectively interpreted as the remnant of a continental volcanic arc derived from subduction of the south-Armorican ocean beneath Gondwana (Oggiano *et al.*, 2010; Pavanetto *et al.*, 2012). The magmatic complex shows large compositional differences within different tectonic units;

such heterogeneity is generally interpreted as primary feature of the volcanic arc (Carmignani *et al.*, 1994b). The 3th sedimentary cycle stands for a major geodynamic change, outlined by shallow-marine pebbly sediments (dubitably referred to the Katian) which were unconformably deposited onto the Ordovician arc (Caradocian Transgression Auct.). During the Hirnantian the sediments became finer grained pelites and sandstones, somewhat intercalated with thin pelagic limestones. A general extensional framework has been proposed for this period (Hirnantian) because of the presence of small volumes of intraplate basalts (Pavanetto *et al.*, 2012). The upper Ordovician succession is generally characterized by a large compositional variability, explained in terms of progressive erosion and dismemberment of the sub-aerial part of an heterogeneous volcanic arc. The following periods (Silurian, Devonian) up to the lower Carboniferous are characterized by homogeneous and stable palaeo-environmental conditions. The Silurian pelagic fossil faunas in fact stand for offshore, though shallow water, sedimentation. Anoxic conditions and scarce feeding of sediments from the main inland are generally recognized. The Silurian succession consists generally of black shales and limestones, with subordinate quartzites, meta-conglomerates, fossiliferous metasilites and marbles; the top of the succession shows a gradational transition to marly meta-limestones and marbles of lower Devonian age. The fourth and last sedimentary cycle (lower Carboniferous) reflect accumulation of clastic sediments within flysch-type successions dominantly characterized by almost homogeneous meta-sandstones.

The structural evolution of the nappe zone has been investigated in several papers over the past 20 years (Carmignani *et al.*, 1978; Conti *et al.*, 1998; Conti *et al.*, 1999; 2001, Table 1). Two main phases of shortening, coeval with low-greenschist metamorphism (Gerrei and Sarrabus Phases, Fig. 2) and nappe stacking have been recognized (Conti *et al.*, 2001). Early deformation was accommodated by N-S shortening that caused development of large isoclinal folds and southward piling of tectonic units. The second phase of shortening (Sarrabus Phase) shows, quite surprisingly, a dramatic change of transport direction from N-S to E over W, well testified by the emplacement of the Sarrabus Unit over the previously stacked units (Fig. 2 - Conti *et al.*, 2001). A third non-metamorphic phase (Flumendosa Phase) restored the early direction of N-S shortening, causing the development of large antiformal structures that refold all previous thrust planes. The limbs of such km-scale structural domes were lately reactivated as normal faults or low-angle detachments during the final extension of the nappe pile (Conti *et al.*, 1999). Although such exhaustive structural dataset, there are no geochronologic constraints on the timing of these events; the only milestone is about placing the beginning of deformation in early Carboniferous (stratigraphic constraints).

3.2. The foreland zone

In the structural framework proposed by Carmignani *et al.* (1979, 1981; 1994), the Iglesias zone represents the most external domain of the Variscan belt exposed in Sardinia. This zone is characterized by very low-grade metamorphism and by folding tectonics associated with development of a steep

schistosity; no significant thrusting events were reported. The effects of Caledonian deformation are somewhat recorded in the pre-Silurian sequences, however these are generally easily distinguishable from the weakly developed Variscan structures.

The Cambrian sedimentary successions of the external zone is, differently from what is seen in the Nappe zone, dominated by shallower epicontinental facies that point out to the existence, since early Cambrian, of a long lasting passive margin located in northern Gondwana. The oldest deposits pertain to the Bithia Fm., which were considered as old as Ediacarian. Recently U/Pb age on detrital zircons (Pavanetto *et al.*, 2012) proved the allochthonous nature of these sediments and support a Cambro-Ordovician age. Hence, the oldest deposits are represented by the Nebida Fm consisting of sandstones with intercalations of dolostones and limestones bearing archaeocyaths faunas. According to Bechstadt and Boni (1994), the Nebida Fm. was deposited in a low gradient omoclinal ramp in shallow marine to tidal flat conditions during lower Cambrian. The change from mainly terrigenous to carbonate sedimentation is marked by the Gonnese group (Pillola *et al.*, 1991), recently subdivided into several formations and members. This group is represented by limestones and dolostones, which were referred to as lower Cambrian on the base of fossil faunas (Archaeocyaths). The Gonnese Group hosts the well known lead and zinc ore deposits, for this reason was also known as "Metallifero" Fm. The deepening of bathymetric conditions related to the sinking of the carbonate platform is testified by the "nodular limestone" re-named Monte Pisano Fm. (Pillola, 1991). This deposit consists of alternating layers of siltite, marls and nodular limestone with trilobites of Mid-Cambrian age. The "nodular Limestone" is capped by the Cabitza Fm. made of siltite; its age is referred to the Mid-Cambrian Lower Ordovician interval on the base of achritarcs, trilobites and graptolites.

After the lower Cambrian, the margin experienced overall emersion and erosion as consequence of the "Sardic Phase", recorded by deposition of thick continental deposits ("Puddinga Fm."). These deposits are considered syn-tectonic pertaining to different system of fan delta (Martini *et al.*, 1991). The Puddinga Fm. (renamed Monte Argentu Fm.) deposited during the same time span that in Nappe zone is represented by the lava flows and lava dome of the calcalkaline magmatic cycle. The first marine deposits unconformably overlying the "Puddinga" fm. are of Upper Caradocian-Ashgillian age, consisting of fossiliferous siltites, and sandstones. They have been studied in detail by Leone *et al.* (1991, 1995), who documented diamictite that testify the onset of the Hirnantian glaciation. The Silurian and Devonian deposits are broadly similar to those of the Nappe zone even if Devonian limestones are poorly represented. Instead, the Culm-like flysch is widely exposed in northern Sulcis area.

The first detailed structural analysis of part of Iglesias zone was carried out by Arthaud (1963), who identified four deformation phases in the Cambrian rocks. A similar deformational sequence was later described also in northern Sulcis by Poll & Zwart (1964), and confirmed in subsequent works (Poll, 1966; Dunnet & Moore, 1969; Arthaud, 1970).

4. The external zones

The basement of Sardinia is widely intruded by granitic plutons of the Corsica-Sardinia batholith (345-285 Ma, Paquette *et al.*, 2003). The majority of plutons belong to the calc-alkaline U2 suite, dated in the range 321-285 Ma (del Moro *et al.*, 1975; Rossi *et al.*, 1993; Paquette *et al.*, 2003; Oggiano *et al.*, 2007). This relatively long time-span reflects two main magmatic episodes, defined on the basis of structural and geochronologic constraints. The first (321-313 Ma, Oggiano *et al.*, 2007; Casini *et al.*, 2012) is closely associated to the anatexis of the metamorphic basement and produced peraluminous granodioritic to monzogranitic plutons (Fig. 4), often emplaced within orogen-parallel shear zones (Cherchi and Musumeci, 1986; Oggiano and Di Pisa, 1988; Casini *et al.*, 2012), or wrench-related structures (Kruhl and Vernon, 2005). After an initial stage of sluggish anatexis driven by muscovite dehydration melting, the volume of melts increase substantially and became more rich in K_2O , feeding large sill-shaped metaluminous plutons, frequently emplaced within NW-SE shear zones (Oggiano *et al.*, 2007; Casini *et al.*, 2012). The second phase of magmatic activity is bracketed between 290-280 Ma (Gaggero *et al.*, 2007; Casini *et al.*, 2012). These young massifs are characterized by relatively small volumes of mafic melts (quartz-diorite, gabbro, tonalite) associated to voluminous felsic rocks. Mafic melts contains hornblende, rare olivine, An30-70 plagioclase, quartz, apatite and Fe/Ti-oxides. Given the major and trace-elements composition of mafic rocks, an origin from the sub-continental mantle can be inferred (Poli & Tommasini, 1999). Felsic terms show instead evidence for extensive contamination caused by mixing between primitive mantle-derived sources and upper crustal melts produced by contact melting (Fig. 7) at shallow levels ($P < 2$ Kbar).



Fig. 7.- Magmatic breccias between "old" granites of the Corsica-Sardinia Batholith (311 Ma, coarse-grained monzogranite) and "young" anatectic granites formed by contact melting around basic complexes dated around 285 Ma (very fine-grained muscovite monzogranite).

5. Stop description Day 6 - The Asinara island

The first day is entirely devoted to the geology of the Asinara island (Fig. 8) The itinerary starts at Fornelli, close to the disembark from Stintino, in the southernmost part of the island, and follows the main road till the lighthouse of Punta Scorno.

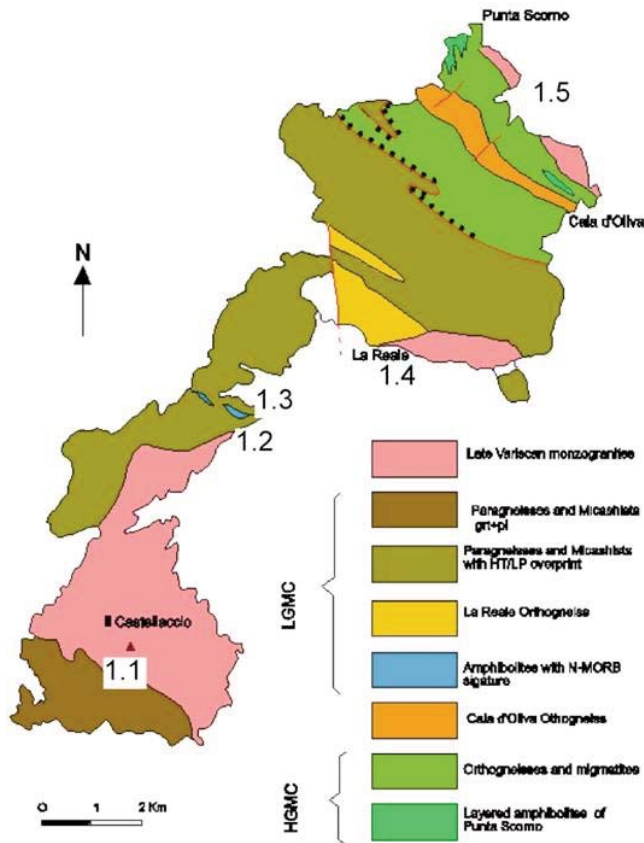


Fig. 8.- Simplified geological map of the Asinara Island.

Stop 6.1. Castellaccio

The contact between Mt. Castellaccio intrusion and the Medium Grade Metamorphic Complex is well exposed on the western cliff.

The Late Variscan Mt. Castellaccio intrusion is made of a porphyritic granodiorite-monzogranite with large laths of K-feldspar (Fig. 9), which underline a N-E striking magmatic flow. Small bodies of nearly equigranular, muscovite-rich monzogranitic facies also occur within the main intrusion (e.g. Cala S. Andrea) and in the northernmost part of the island.

Oligoclase-bearing paragneisses and micaschists are mainly affected by the F2 tight to isoclinal folds. It is worth to note that no meaningful contact metamorphism occur either in schist close to the contact neither in the schists and paragneisses septa embedded within the granite.

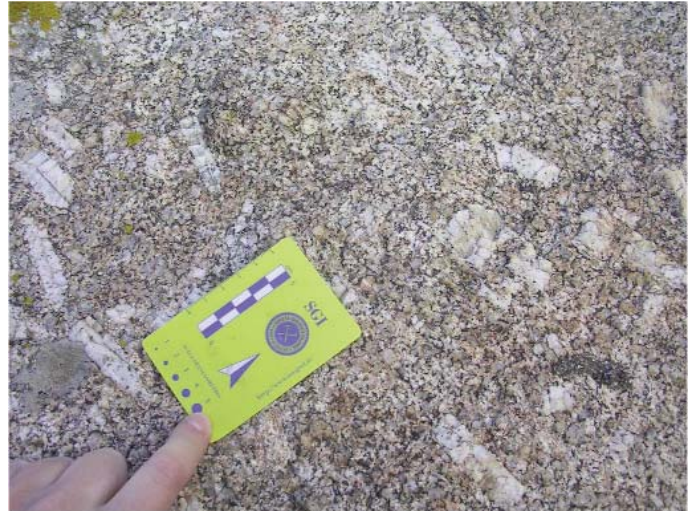


Fig. 9.- Monzogranite of Castellaccio intrusion.

Stop 6.2. Micaschists and paragneisses with HT imprint

Moving to Cala d'Oliva, some hundred meters northward of the contact of the Castellaccio intrusion, the effect of HT/LP metamorphism overprinting the previous Barrovian one is well visible within the Medium Grade Metamorphic Complex. Two main deformation phases (D2 and D3, Carosi *et al.*, 2004) give rise to interference figures visible on the road cut. In Li Stretti zone clear relationship between S1 that is parallel to S0, D2 tight folds and upright D3 folds are showed (Fig. 10). Pegmatite dykes intrude the MGMC both sub-parallel to the S2 schistosity and folded by D3, other cut through the schistosity, suggesting the existence of at least two intrusive events. The HT/LP overprint is characterized by static crystallization of cm-size andalusite crystals (Fig. 11) overprinting the D3 deformation phase (Fig. 12). Andalusite overgrows and rims previous staurolite sinkynematic porphyroblasts according to the decompressive reaction: $St + Ms + Qtz = And + Bt + H_2O$.



Fig. 10.- Type 3 Interference pattern between F2 and F3 (upright folds).

The L2 stretching lineation is well developed in the quartzites and it is nearly parallel to the F2 fold axes.



Fig. 11.- Chialstolite at Punta la Nave outcrop.



Fig. 14.- Mineral assemblage within amphibolite boudins.

Stop 6.4. La Reale high-strained orthogneiss

Close to La Reale, a continuous transition between an orthogneiss and 'orthomicaschists' is exposed. The transition proceeds along with the deformation and the development of a plano-linear fabric defined by quartz-feldspar aggregate ending into a micaschist with quartz ribbons and garnet in a matrix of fine plagioclase, biotite and muscovite and fibrolite which generate at the expense of biotite (Fig. 15) according to reactions apparently referable to base-cation leaching such as $2K(Mg, Fe)AlSi_3O_{10}(OH)_2 + 14H^+ = Al_2SiO_5 + 2K^+ + 6(Mg, Fe)_2^+ + 9H_2O + 5SiO_2$. They appear to be triggered by high-strain concentration as they are confined within shear zones where also quartz and micas show the effect of extensive deformation.



Fig. 15.- Fibrolite growing after biotite (La Reale orthomicaschists).

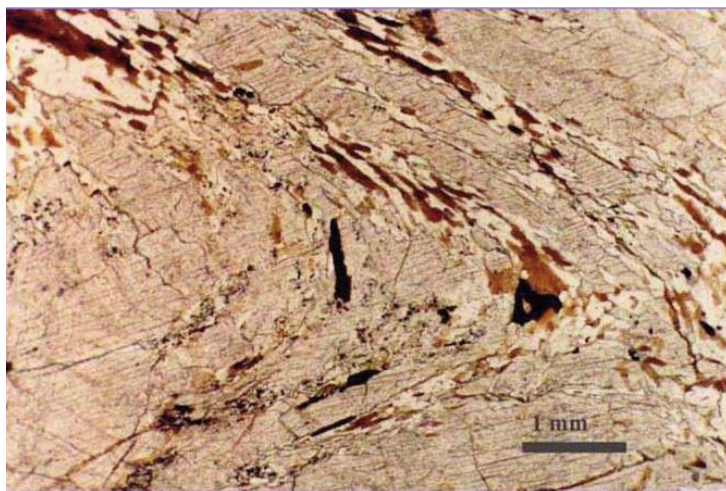


Fig. 12.- D3 crenulation overgrown by wide andalusite porphyroblast.

Stop 6.3. Amphibolitic boudins at 'Li Stretti'

Boudins or lenticular bodies of decametric size massive amphibolites (N-morb type) are well exposed on the cliff (Fig. 13), associated with light-grey quartzites. The mineral assemblage mainly consists of hornblende and plagioclase with minor biotite, clorite and oxides (Fig. 14) . According to Cappelli *et al.* (1992) the protholith of the amphibolites are N-MORB basalts of unknown age. The age of the HT/LP metamorphism is 303 My (Ar/Ar on hornblende)



Fig. 13.- Amphibolite boudins, "Li Stretti".

Stop 6.5. Cala d'Oliva - Punta Scorno orthogneiss

We get through the High Grade Metamorphic Complex, mainly composed of migmatitic gneiss, orthogenesis, metatexite and diatexite.

The Cala d' Oliva orthogneiss is a tabular body with variable thickness (protolith age is 432 My, U-Pb zircon). The orthogneiss edges are interlayered with discontinuous, mica-rich, domains mostly composed of biotite + muscovite that show enrichment in sillimanite and cordierite grown during the late HT/LP metamorphic event. On the S2 schistosity the stretching lineation is down-dip and kinematic indicators suggest a top to the SE sense of shear. The orthogneiss is

wrapped by an alternation of augen-gneiss and mylonitic micaschists. Diatexites exposed northward are characterized by either stromatic, nebulitic and agmatitic textures. Restitic palaeosomes and amphibolitic bodies preserving a polyphase deformation history (almost two folding phase) are exposed within diatexites.

Punta Scorno

The Punta Scorno orthogneiss is a mylonitic augen gneiss. The mineral assemblage is the same of the Cala d'Oliva orthogneiss even if mica, garnet and sillimanite are comparatively more abundant.

The main characteristic is the occurrence of meter-thick levels rich of cm to dm-sized k-feldspar porphyroclasts with asymmetric recrystallized tails (visible at the naked eye) pointing out a top to the south sense of shear with. Nice examples of porphyroclasts, rotated both in the XY and XZ principal planes. The large laths of alkali feldspar exhibit both oblate shapes that turn into plan-linear within short distance, testifying for low-scale strain partition. In the late case the stretching lineation lays down dip (Fig. 16).



Fig. 17.- Punta Scorno white leptynite alternating dark amphibolite on the cliff.

Hectometric outcrops of banded amphibolites are exposed on the northwestern cliff, south of the lighthouse. These leptyno-amphibolic outcrops (Fig. 17) consist of cm-thick amphibolites alternated with leptynitic layers. Leptynites are trondjemitoid in composition with composite plagioclase, quartz and garnet.



Fig. 16.- Punta scorno Orthogneiss. Notice the different strain pattern affecting the big k-feldspar porphyroclasts.

Relic assemblages of clinopyroxene + garnet+ plagioclase testify for a high to intermediate P granulite facies metamorphic event (Di Pisa *et al.*, 1993; Carosi *et al.*, 2004).

Under the lighthouse, agmatites contain lumps of banded amphibolite and restite. Here remarkable post-D2, syn-anatexis high temperature shear zones are exposed. Rotated enclaves of dark amphibolites and tailed restites show non-univocal shear sense.

References

Carosi R., Di Pisa A., Iacopini D., Montomoli C., Oggiano G. (2004) - The structural evolution of the Asinara Island (NW Sardinia, Italy). *Geodinamica Acta* 17/5 (2004) 309-329.

Di Pisa A., Oggiano G., Talarico F. (1993) - Post collisional tectono-metamorphic evolution in the axial zone of the Hercynian belt in Sardinia: the example from the Asinara island. Orleans, Doc. BRGM 219 (1993), 216-217.

Day 6 - plan B (in case of heavy sea)

The Posada-Asinara Zone (PAL)

Stop 6-1b: the Posada-Asinara mylonitic shear zone (PAL)

Close to the Giuncana village: sheared micaschists and paragneisses (muscovite + biotite + plagioclase + garnet + staurolite ± kyanite) of the Medium Grade Metamorphic Complex (Carmignani *et al.*, 1994). Mineral compositions show evidence for nearly isothermal decompression from 0.9 GPa and 630°C to 0.4 GPa and 540°C (Casini *et al.*, 2009; Frassi *et al.*, 2009). The age of metamorphic events is constrained between 340-325 Ma for the HP event (Rb/Sr muscovite, U-Pb zircon and Th-Pb monazite, Carosi *et al.*, 2011), and around 300 Ma (Rb/Sr muscovite) for the later re-equilibration.

Stop 6-2b: Amphibolite with eclogite assemblage

Outcrop of eclogite boudins derived from N-MORB basalts (inferred PT condition of the eclogitic event 1.4 GPa, 600°C, Cortesogno *et al.*, 2004) embedded within highly deformed micaschists some 300 mt from the high-strain zone of the PAL.

Stop 6-3b: The Badesi syntectonic granodiorite

The Badesi pluton is a syntectonic granodiorite (300.1 ± 6.1 Ma crystallization age) emplaced within the PAL. The pluton is roughly elongated along a NNW-SSE direction and consists of medium-grained hornblende-granodiorite. The fabric is well perceptible in a small quarry near La Tozza village (Fig. 18). The main foliation, evidenced by high-strained biotite + amphibole folic enclaves, is parallel to the shear zone boundaries. The foliation vanishes toward the core of the pluton, near the Trinità village, where a primary magmatic fabric defined by oriented large k-feldspar phenocrysts and amphiboles is observed. This argues for melt-present deformation, which is also confirmed, at the thin section scale, by syn-magmatic fracturing of plagioclase (Fig. 19).



Fig. 18.- High-strained mafic enclaves within the peripheral part of the Badesi Granodiorite.

Stop 6-4b: The migmatitic complex

The High Grade Migmatitic Complex at Lu Pottidolu-Pta Bianca. Along the path starting on the northern side of the beach, several well polished outcrops of metatexite, diatexite

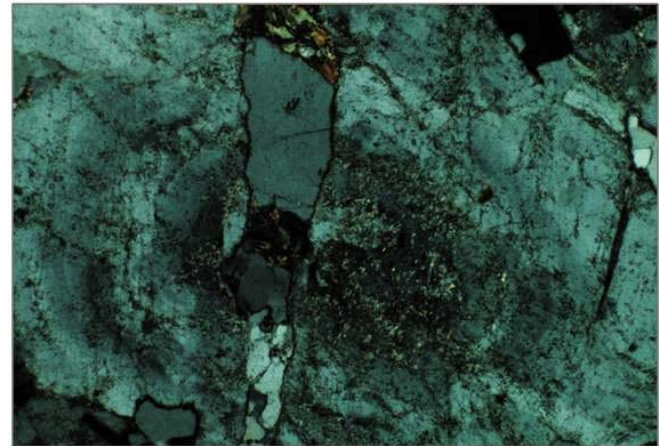
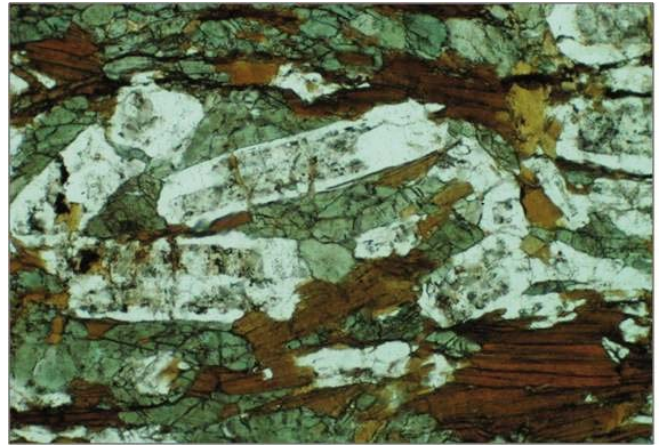


Fig. 19.- (a) fracture in plagioclase filled with amphibole + quartz; (b) fracture in zoned plagioclase filled with Na-rich plagioclase + quartz. Note that fractures do not propagate outside the phenocrysts.

and syntectonic granodiorite. The Pta Bianca migmatites represents the western tip of the large granodioritic peraluminous Barrabisa pluton (Fig. 20). From the small beach, the path gets through metatexite characterized by low melt/protolith ratio (< 20 % melt) to diatexite (20-90 % melt) and syntectonic granodiorite for increasing melting rates. Leucosomes in metatexite are trondhjemitic, mainly composed of biotite + plagioclase + quartz + apatite ± cordierite ± garnet ± muscovite). K-feldspar tends to increase in diatexites, for increasing melt/protolith ratios. The PT paths that assisted the transition from metatexite to diatexite is schematically drawn in Fig. 21.

Stop 6-5b: Emplacement fabric of the Barrabisa peraluminous pluton (~313 Ma)

In a small peninsula one km north of Pto Pollo (Fig. 20) it is notably exposed the peraluminous granodiorite part of the Barrabisa pluton. On the well-polished reef around the beach, biotite schlieren and quartz-rich layers mark the emplacement fabric. At a closer examination, it is perceptible that the fabric should reflect a component of sub-magmatic to solid-state flow, as evidenced by fracturing of some large k-feldspar porphyroclast and recrystallization of quartz into incipient polycrystalline ribbons.

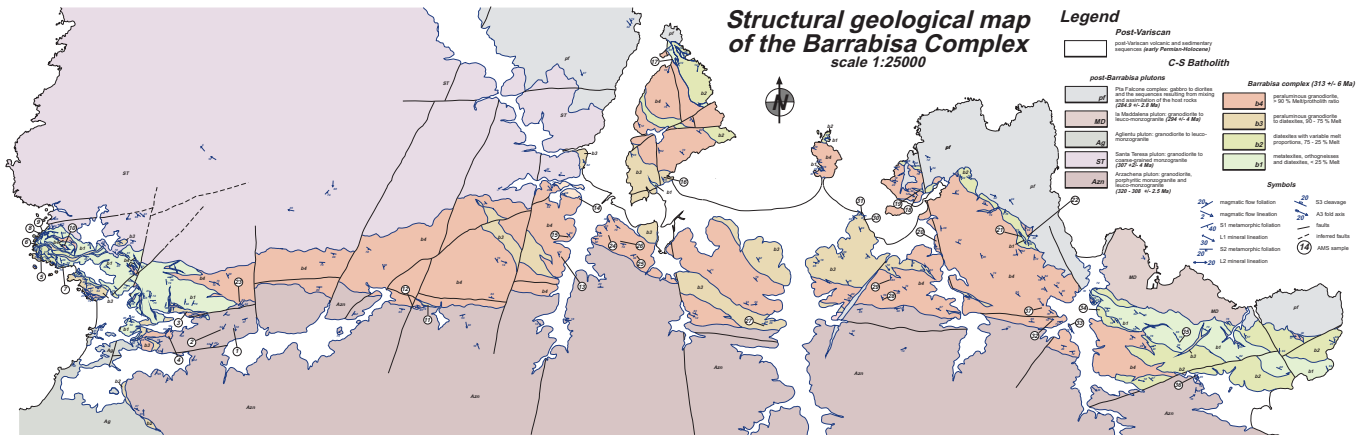


Fig. 20.- Structural map of the Barrabisa Granite (N-Sardinia).

P[GPa]

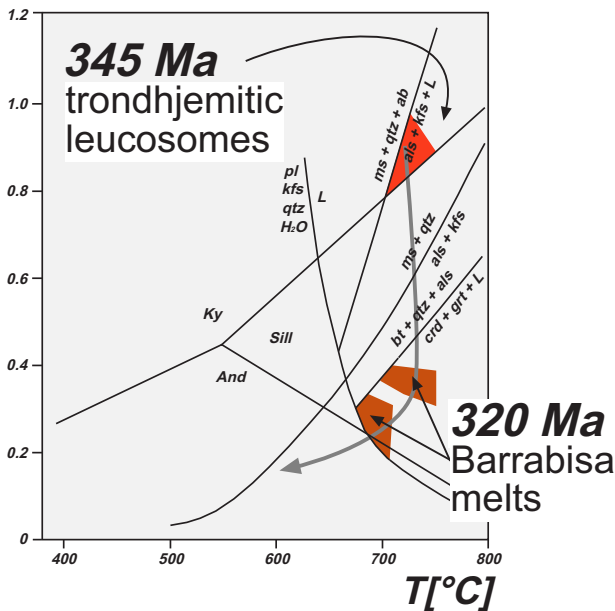


Fig. 21.- PT path of Barrabisa melts.

References

Cappelli B., Carmignani L., Castorina F., Di Pisa A., Oggiano G., Petrini R. (1992) - A Variscan suture zone in Sardinia: geological and geochemical evidence, Paleozoic Orogenies in Europe special issue), *Geodin. Acta*, **5** (1-2), 101-118.

Carmignani L., Barca S., Disperati L., Fantozzi P., Funedda A., Oggiano G., Pasci S. (1994) - Tertiary compression and extension in the Sardinian basement. *Boll. Geof. Teor. Appl.*, **36**, 45-62, Trieste.

Carosi R., Frassi C., Montomoli C. (2009) - Deformation during exhumation of medium- and high-grade metamorphic rocks in the Variscan chain in northern Sardinia (Italy). *Geological Journal*, **44** (2009), pp. 280-305.

Carosi R., Montomoli C., Tiepolo M. & Frassi C. (2011) - Geochronological constrains on post-collisional shear zones in the variscides of Sardinia (Italy). *Terranova*. Volume 24, Issue 1, pages 42–51, February 2012. DOI: 10.1111/j.1365-3121.2011.01035.

Casini L. & Oggiano G. (2008) - Late orogenic collapse and thermal doming in the northern Gondwana margin incorporated in the Variscan Chain: a case study from the Ozieri Metamorphic Complex, northern Sardinia, Italy. *Gondwana Research*, vol. 13 (3), p. 396-406. ISSN 1342-937X.

Casini L., Funedda A., Oggiano G. (2010) - A Balanced foreland-hinterland deformation model for the Southern Variscan belt of Sardinia, Italy. *Geological Journal*, vol. 45 (5-6), p. 634-649. eISSN 1099-1034.

Casini L., Cuccuru S., Maino M., Oggiano G. Tiepolo M. (2012) - Emplacement of the Arzachena Pluton (Corsica-Sardinia Batholith) and the geodynamics of incoming Pangaea. *Tectonophysics*, in press doi: 10.1016/j.tecto.2012.03.028

Cherchi G.P., Musumeci G. (1986) - Il leucogranito de M. Grighini (Sardegna centro-occidentale), un esempio di granito deformato all'interno di una fascia di taglio duttile: caratteristiche meso e microstrutturali. *Atti della Societa Toscana di Scienze Naturali Residente in Pisa, Memorie, Processi Verbali, Serie A* ISSN 0365-7655 1986, vol. 93, p. 13-29 (16 ref.)

Conti P., Carmignani L., Oggiano G., Funedda A., Eltrudis A. (1999) - From thickening to extension in the Variscan belt - kinematic evidence from Sardinia (Italy). *Terra Nova*, vol. 11, Issue 2-3, p. 93–99, April/June 1999

Conti P., Funedda A. e Cerbai N. (1998) - Mylonite development in the Hercynian basement of Sardinia (Italy). *Journal of Structural Geology*, vol. 20, n° 2/3, 121-133. Oxford.

Conti P., Carmignani L., Funedda A. (2001) - Change of nappe transport direction during the Variscan collisional evolution of central-southern Sardinia (Italy). *Tectonophysics*, v. 332, p. 255-273.

Cortesogno L., Gaggero L., Oggiano G, Paquette J.L. (2004) - Different tectono-thermal evolutionary paths in eclogitic rocks from the axial zone of the Variscan Chain in Sardinia (Italy) compared with the Ligurian Alps. *Ofoliti* **29** (2):125-144.

Cruciani G., Franceschelli M., Elter F.M., Puxeddu M., Utzeri D. (2008) - Petrogenesis of Al-silicate-bearing trondhjemitic migmatites from NE Sardinia, Italy. *Lithos*, **102**, 554-574.

Cruciani G., Franceschelli M., Jung S., Puxeddu M., Utzeri D. (2008) - Amphibole- bearing migmatite from Variscan Belt of NE Sardinia, Italy: partial melting of a mid-Ordovician igneous source. *Lithos*, **102**, 208-224.

Di Vincenzo G., Carosi R., Palmeri R. (2004) - The relationship between tectono-metamorphic evolution and argon isotope records in white mica: constraints from in situ 40Ar-39Ar laser analysis of the Variscan basement of Sardinia. *Jour. Petr.* **45**, 1013-1043.

Ferrara G., Ricci C.A., Rita F. (1978) - Isotopic ages and tectono-metamorphic history of the metamorphic basement of north-eastern Sardinia. *Contr. Min. Petr.*, **68**: 99-106, Berlin.

Ferré E.C., Leake B.E. (2001) - Geodynamic significance of early orogenic high-K crustal and mantle melts: example of the Corsica Batholith. *Lithos*, **59**, 47-67.

Frassi C., Carosi R., Montomoli C., Law R.D. (2009) - Kinematics and vorticity of flow associated with post-collisional oblique transpression in the Variscan Inner Zone of northern Sardinia (Italy). *Journal of Structural Geology* **31**, 1458-1471.

- Giacomini F., Bomparola R., Ghezzi C., Gulbrandsen H. (2006) - The geodynamic evolution of the Southern European Variscides: constraints from the U/Pb geochronology and geochemistry of the lower Palaeozoic magmatic-sedimentary sequences of Sardinia (Italy). *Contrib. Mineral. Petrol.* **152**, 19-24.
- Giacomini F., Bomparola R.M., Ghezzi C. (2005) - Petrology and geochronology of metabasites with eclogite facies relics from NE Sardinia: constraints for the Palaeozoic evolution of Southern Europe. *Lithos*, **82**, p. 221-248.
- Giacomini F., Dallai L., Carminati E., Tiepolo M., Ghezzi C. (2008) - Exhumation of a Variscan orogenic complex: insights into the composite granulitic-amphibolitic metamorphic basement of south-east Corsica (France). *Journal of Metamorphic Geology*. Volume 26, Issue 4, pages 403-436, May 2008.
- Kruhl J.H., Vernon R.S. (2005) - Syndeformational emplacement of a tonalitic sheet complex in a late-Variscan thrust regime: fabrics and mechanism of intrusion, Monte'e Senes, northeastern Sardinia, Can. Min. **43** (2005) 387-407.
- Macera P., Di Pisa A., Gasperini D. (2011) - Geochemical and Sr-Nd isotope disequilibria during multi-stage anatexis in a metasedimentary Hercynian crust., *European Journal of Mineralogy: an International Journal of Mineralogy, Geochemistry and related Sciences*, vol. 23, p. 207, tot. pag. 16, tot. autori 3, 2011.
- Oggiano G., Di Pisa A. (1988) - I graniti peralluminosi sin-tettonici nell'area di Trinità d'Agultu e i loro rapporti con le metamorfite di alto grado della Bassa Gallura (Sardegna settentrionale) *Boll.Soc. Geol. It.* **107**, 471-480.
- Oggiano G., Casini L., Rossi P., Mameli P. (2007) - Long lived dextral strike-slip tectonics in the southern Variscan Belt: evidence from two syn-kinematic intrusions in north Sardinia. *Geologie de la France (Meeting on Mechanics of Variscan Orogeny: a modern view on orogenic research Orleans 13-15 2007)*, **2**, 141.
- Oggiano G., Cherchi G.P., Aversano A., Di Pisa A., Ulzega A., Orrù P., Pintus C. (2005) - Note illustrative della Carta Geologia d'Italia, Foglio 428 Arzachena. Firenze: S.E.L.C.A.
- Palmeri R., Fanning M., Franceschelli M., Memmi I., Ricci C.A. (2004) - Shrimp dating of zircons in eclogite from the Hercynian basement from north eastern Sardinia (Italy). *Neues Jahrbuch. Fur Mineralogie Monatshefte* **6**, 275-288.
- Paquette J.-L., Ménot R.-P., Pin C., Orsini J.-B. (2003) - Episodic short-lived granitic pulses in a post-collisional setting: evidence from precise U-Pb zircon dating through a crustal cross-section in Corsica. *Chem. Geol.* **198** (2003) 1-20.
- Poli G., Tommasini S. (1999) - Insights on acid-basic magma interaction from the Sardinia-Corsica batholith: the case study of Sarrabus, southeastern Sardinia, Italy. *Lithos*, **46** (3), 553-571.
- Rossi P., Cocherie A. (1991) - Genesis of a Variscan batholith. Field, petrological and mineralogical evidence from the Corsica-Sardinia batholith, in: Freeman R., Huch M., Mueller St. (Eds) *The European Geotraverse part 7, Tectonophysics* **195** 319-346.
- Rossi P., Durand-Delga M. & Cocherie A. (1993) - Caractère volcano-plutonique du magmatisme calco-alcalin composite d'âge Stéphanien supérieur-Permien inférieur en Corse. *C. R. Acad. Sci. Paris, Série II*: p. 1779-1788, Paris.
- Rossi Ph., Oggiano G., Cocherie A. (2009) - A restored section of the 'southern Variscan Realm' across the Corsica-Sardinia microcontinent. *C. R. Geosc.* **341**, 224-238.

Day 7: The Ordovician magmatic arc

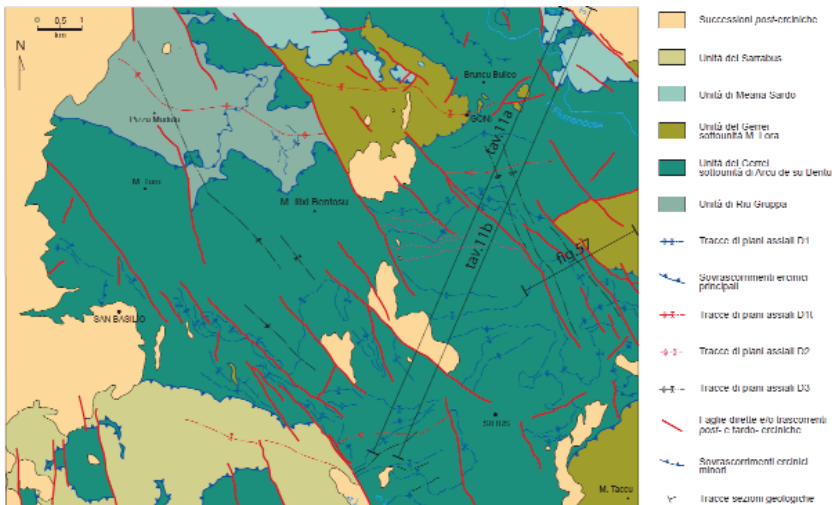


Fig. 22.- Structural sketch map of the Goni area (Funedda et al., in press).

Leaving the state road SS131 at 40 km from Cagliari, we turn towards the east and we will reach the village of Senorbi; then, we get to the small village of San Basilio that is located exactly at the contact between the Cainozoic cover and the Variscan basement (Fig. 22). From San Basilio, we move once again eastward to the Silius area along the district road to Goni, and after one kilometre we walk on a plateau constituted by Middle -Upper Ordovician volcanic rocks called "Porfiroidi". We stop along the road close to Perdusai region.

Stop 7.1: Middle Upper Ordovician Volcanic rocks

Along the northern side of the road crops out a rocks made up by large (up to 5 cm) phenocrysts of pinkish K-feldspar, that still preserve a typical euhedral habit with also smaller phenocrysts of quartz, all surrounded by a phyllitic matrix, generally greenish, affected by a disjunctive cleavage, developed in very-low grade metamorphic condition (Fig. 23). Chemical analyses on specimens sampled in this and other neighbouring outcrops show a rhyolite-rhyodacite composition (Fig. 24)



Fig. 23.- Stretched meta-rhyolite with large k-feldspar porphyroclasts.

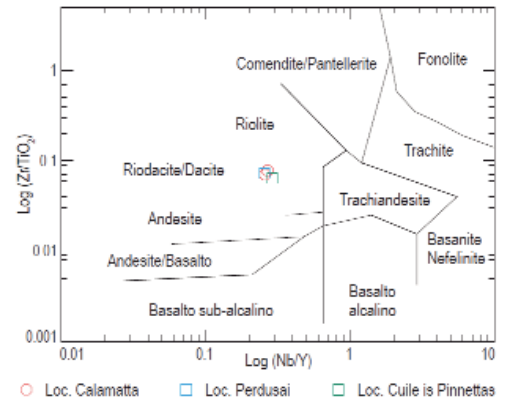


Fig. 24.- Chemical composition of 'Porphyroids'.

Stop 7.2: Variscan D1 structures

We then continue to move eastwards and when we reach the crossroad we turn towards Silius. Along the road we cross several small isoclinal folds related to the Variscan D1 shortening phase that involve both the Porfiroidi and their Upper Ordovician sedimentary cover (the Metarcose di Genna Mesa and the Argilloscisti di Rio Canoni). Just few meters after the crossroad crops out a small syncline with Hirnantian fossiliferous shale at the core, and after 1 km a small anticline with a the core the Porfiroidi, but in this case characterized by small (up to 1 cm) phenocrysts of k-feldspar. Along a road cut is possible to see a normal limb whit at the base the volcanic rocks, than moving upwards)thus to the east, crop out the metasandstones of the Metarcose di Genna Mesa fm. and the fossiliferous shales of the Argilloscisti di Rio Canoni. The contact between these formation are generally sheared because the strong deformation suffered, they are smaller range structures of larger, isoclinal, recumbent folds with km-size amplitude, facing to the south-southwest, and with axes trending NNW (Fig. 25), that constitute a nappe-like structure (Fig. 26).

The same small folds are crosscut several times by the same road before to reach the Silius village. Then, we move to Villasalto village.

Stop 7.3: Su Suergiu mine (Villasalto): the Villasalto overthrust

The Villasalto overthrust, previously known as "Villasalto fault" (Teichmüller, 1931; Calvino, 1960), is one of the most important Variscan tectonic feature in SE Sardinia. It crops out for 40 km, running roughly E-W, from the Tyrrhenian coast in the east, near capo San Lorenzo, to the eastern border of the Miocene rift near Monte Grighini in the west. Recently has been interpreted as an overthrust surface of regional importance, produced during the shortening event of Variscan orogeny (Carmignani and Pertusati, 1977; Carmignani et al., 1978). Along this surface the Sarrabus Unit is thrust over the Gerrei Unit (Fig. 27) and a foliated cataclasites (Fig. 28), up to 300 m thick, made up mainly by Silurian shale fragments, developed. Inside the cataclastic belt big slices are incorpo-

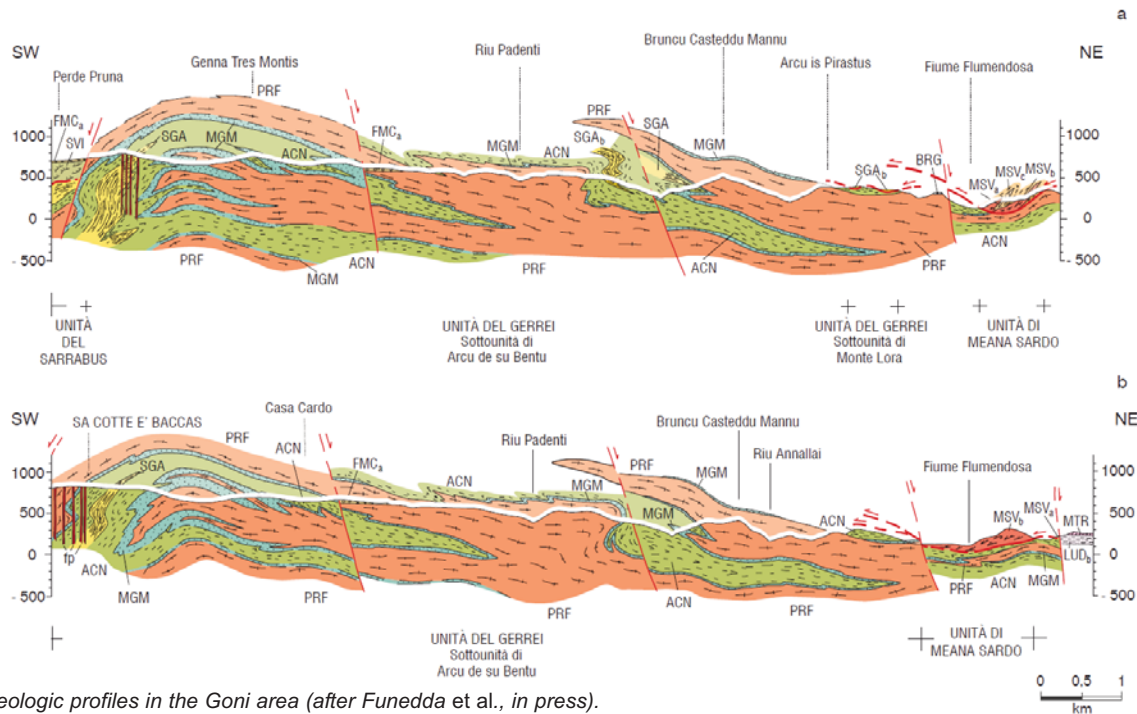


Fig. 25.- Geologic profiles in the Goni area (after Funedda et al., in press).

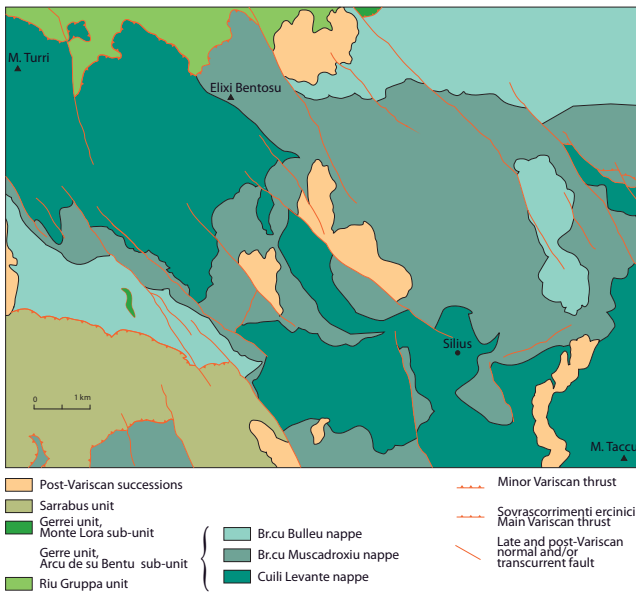


Fig. 26.- a) Simplified structural map of the Goni area.

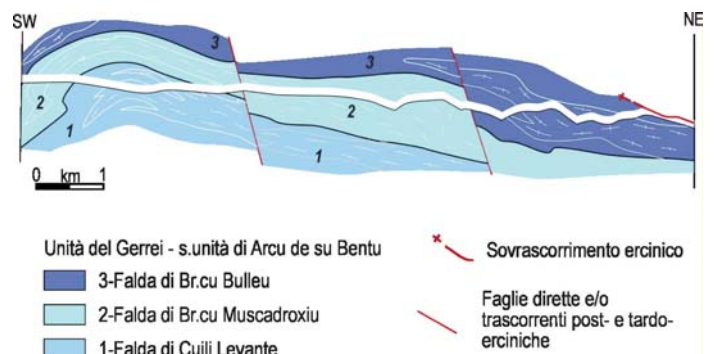


Fig. 26.- b) simplified cross-section (after Funedda et al., in press).

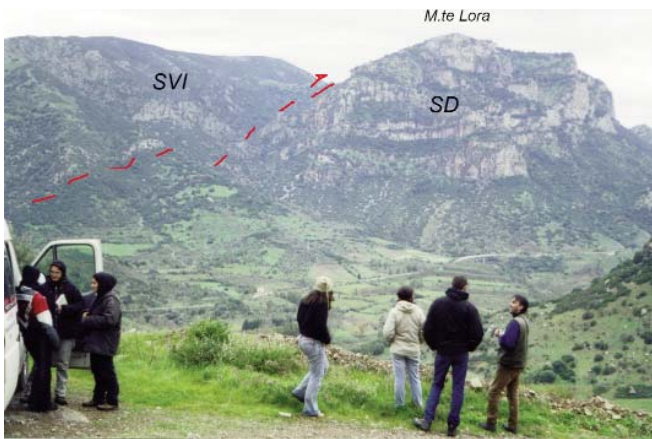


Fig. 27.- The Villasalto thrust.

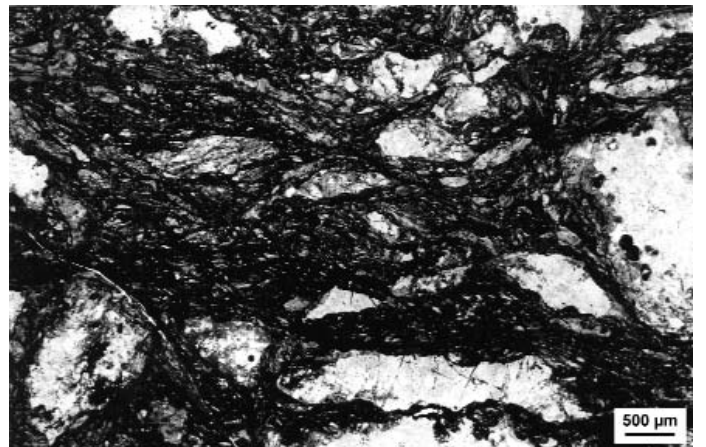


Fig. 28.- Details of the cataclasite deformed within the Villasalto shear zone.

rated, sometimes with size up to 500 m, derived from the surrounding formations. The analysis of kinematic indicators along the thrust surface indicated a “top to the west” transport direction, which predate the emplacement of the lower tectonic units (Gerrei, Meana Sardo and Riu Gruppa-Castello Medusa Units) (Fig. 29).

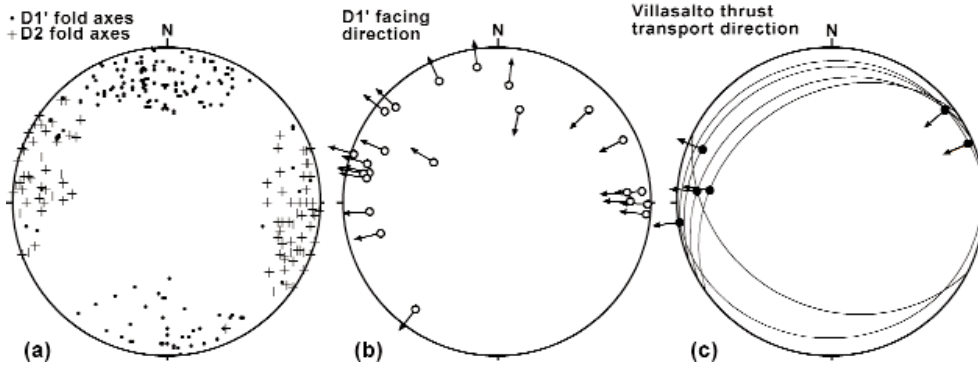


Fig. 29.- Trend of kinematic indicators, Villasalto thrust.

Microstructural analysis (Conti and Patta, 1998) show that cataclastic flow was the primary deformation mechanism and produced fine-grained foliated black cataclasites, with larger quartz and feldspar porphyroclasts; evidence for low temperature crystal plasticity (undulose extinction, deformation bands and subgrain rotation) is restricted to large quartz porphyroclasts. The younger rocks of the underlying tectonic unit (Gerrei Unit) involved are Culm-like clastic deposits aged Lower Carboniferous (Barca and Olivieri, 1991).

The present-day geometry of the Villasalto Overthrust, generally dipping towards south, has been reached during the last movements of the Variscan shortening phase. The same that are responsible of the large antiform and synform framework of the nappes stack in the Flumendosa area. Often the Villasalto overthrust, as well as most of the D1 structures in SE Sardinia, has been reactivated as normal fault during post-collisional extension. Even during extension the Villasalto Overthrust has been involved in asymmetrical folds with large overturned limbs, so locally, its surface dip towards north. Furthermore the Villasalto Overthrust is locally cross-cut by normal faults both late Paleozoic and “Alpine” in age.

The stop is near the Villasalto village, close to the ancient “Su Suergiu” mine, where the overthrust is well exposed and where, for the first time, it was recognized because the mining activities for lead and antimony ore. There the Cambrian-Lower Ordovician metasandstones of the base of Sarrabus Unit overlie the upper Devonian metalimestones of the Gerrei Unit. In the between a wide cataclastic belt is exposed, made up by fragments of Silurian black shales, metamorphic quartz veins, often strongly deformed, and big boulders of porfiroidi, metalimestones and Cambrian-Lower Ordovician metasandstones.

Stop 7.4: Monte Perdosu: Ordovician succession of the Gerrei tectonic unit (after Carnignani *et al.*, 1986, modified)

We move across Villasalto village down to the Flumendosa valley, the local road pass through the wide cataclastic zone of the Villasalto thrust and going down to the valley, we pass through Siluro-Devonian succession of the Gerrei tectonic unit. The stop 2.4 is easily reached after a short walk on the state road SS559. Eastward from the M. Ferru relief is possible to observe the pre-Upper Ordovician succession of the M. Lora sub-unit that overthrust the Arcu de Su Bentu sub-unit. Both are part of the Gerrei unit.

Walking by foot along a short trail on the Flumendosa river, we pass through the following formations belonging to the Monte Lora sub-unit, from the top (Fig. 30, Fig. 31):



Fig. 30.- Landscape along the Flumendosa river.

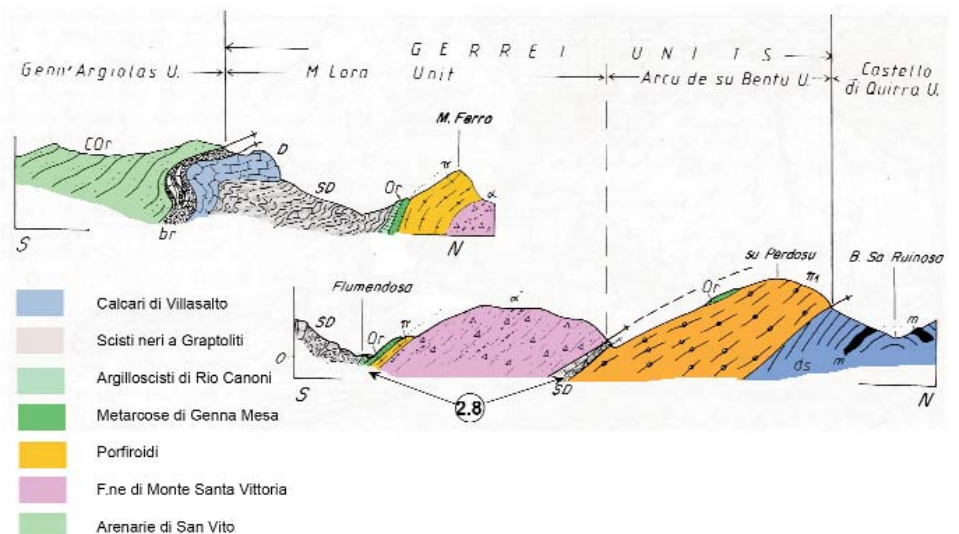


Fig. 31.- Cross sections through the Flumendosa antiform (after Carnignani *et al.*, 1986).

- 1) feldspathic quartzites and meta-sandstones just below the fossiliferous slates of Rio Canoni fm (Upper Ordovician).
- 2) Augen meta-volcanic rocks (Porfiroidi fm), presumably derived from primary pyroclastic deposits; composition ranges from rhyolite to rhyodacite;
- 3) metasediments including micaceous meta-sandstones, meta-conglomerates and quartzites derived from sedimentary reworking of former volcanic rocks (Su Muzziioni fm).
- 4) basic and intermediate meta-volcanic rocks (Mt Santa Vittoria fm).

The thrust which juxtaposes this sequence above the Arcu de Su Bentu Unit is observable along the path close to the stream flowing down from the Mt. Su Perdosu. The tectonic contact is marked by a thin layer of black phyllites hosting Silurian-Devonian lenses of marbles, which represents the sedimentary cover of Porfiroidi fm within the Arcu de Su Bentu Unit.

Stop 7.5: Porto Corallo: Arenarie di San Vito fm, overturned limbs of Variscan isoclinal folds

The meta-sandstones of S. Vito fm (Sarrabus Unit, the roof of Villasalto thrust) are exposed along the beach below the quaternary sediments. The rocks are essentially fine grained meta-sandstones organized into thin (50 cm thick) strata characterized by cross-bedding, load casts, and flute-casts (Fig. 32). The polarity - still detectable - indicates the overturning of the original sedimentary succession. The S1 Variscan foliation is poorly developed within coarse-grained terms, while it is more pervasive within pelitic layers. Intersection lineations L0-1 suggest that fold axes are oriented about N-S, whereas the relationships between S0, S1 and the fold axes evidence a W-directed facing direction. As once proposed by Carmignani & Pertusati (1977) the overturned sequence - exposed for some 800 m along the coast - represents the overturned limb of a large antiformal whose axial plane dips toward E; the normal limb is instead exposed on the hills some hundreds of m W to the coastline, in the Br.cu 'e Mesu area (Carmignani & Pertusati, 1977; Carmignani *et al.*, 1986; Conti & Patta, 1998, Fig. 33).



Fig. 32.- Sedimentary structures in the S. Vito formation.

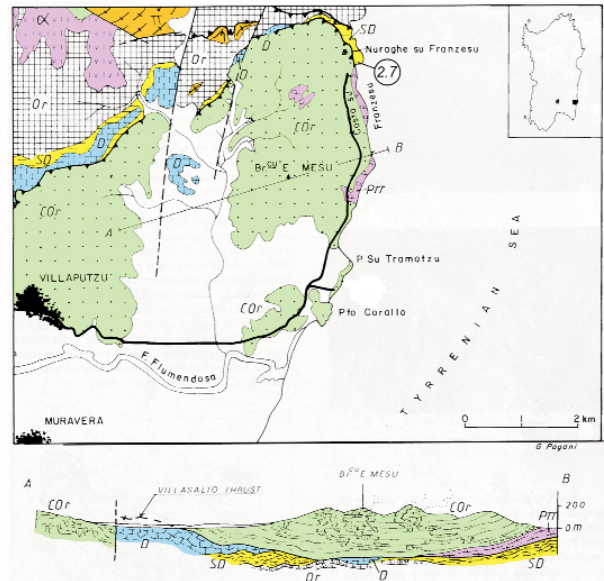


Fig. 33.- Sketch map of the Porto corallo area (after Carmignani *et al.*, 1986).

Day 8: The Sardinic unconformity

From Iglesias we go to the west through the national road SS 130.

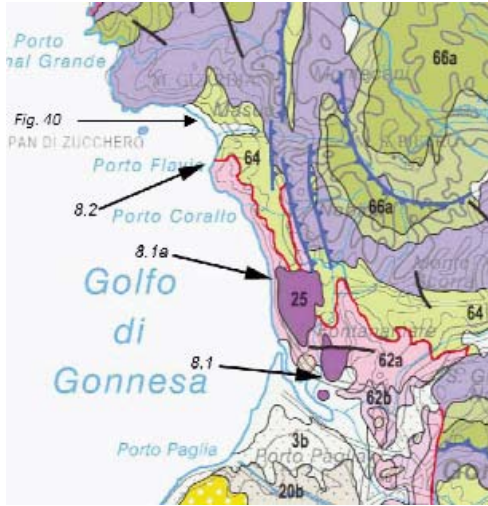


Fig. 34.- Location of stops of the day 8, in red is the Sardinic unconformity (map from Carmignani et al., 2008).

Stop 8.1: The Upper Carboniferous San Giorgio Basin (the oldest sediments not affected by Variscan metamorphism)

Near Iglesias, after the road tunnel (Fig. 34), there is a good exposition of the Middle Cambrian-Lower Ordovician Cabitza Fm. unconformably capped by a post-Variscan deposit of Upper Carboniferous age. The unconformity basal contact is erosional and some small channels are evident near the base. It is a mainly silicoclastic sedimentary succession, from bottom to top:

- the very base consists of a 10 m of polygenic conglomerate, well cemented, with clasts derived from the Cambrian dolostone and limestone that forms the surrounding hills;
- dolostone with alternating sandstone and microconglomerate, about 15 m thick, well stratified, where a meter-thick interval with tetrapod footprints has been described (Fondi, 1979);
- 5 m of shale and carbonaceous marls with abundant fossil plants (Pittau *et al.*, 2008 and references therein);
- the succession is terminated by 15 m of conglomerate, with sandstone containing leaves and tree-trunks.

The exact geometry of this small basin is not clear because it is partially eroded or covered by waste deposits of the Campo Pisano Mine. The basin rests on the core of an exhumed Variscan synformal syncline (Cabitza syncline). No evidence exists regarding basin boundary faults, suggesting that by Late Carboniferous, the Variscan basement of the external zone had been exhumed and that it was a depressed area where lacustrine and fluvial sediments were accumulating.

Stop 8.1 (alternative): non conformity between Variscan basement and Triassic cover near Campumari

Along the road to Nebida (Fig. 34), that run close the cli. on the sea, crops out the base of the Triassic cover (Barca & Costamagna, 2003). At the very base is a silici-clastic succession (polymict conglomerates, coarse sandstones and a reddish plaeosol) that to the top pass to carbonatic rocks (dolostones and dolomitic limestones) (Fig. 35).

The conglomerates are clast supported, crude stratified in metric beds, the matrix is generally arenaceous, sometimes dolomitic (Fig. 36). Clasts are up to 10 cm, from sharp to rounded, are made by Cambrian dolostones, Ordovician siltstones and Silurian limestones. The dolomitic limestones are generally poorly bedded rarely with a fissile lamination. Locally there are breccias and dissolution voids. Probably the deposition occurred in a delta fan with cyclic emersions in hot-dry climatic conditions.

The Triassic sediments non-conformably overlie the oldest post-sardic succession: the Monte Argentu Formation (also called Puddinga ordoviciana according the ancient authors).



Fig. 35.- Non-conformity between Variscan basement and Triassic cover near to Campumari (Stop 8.1 alternative), see location in Fig. 37.



Fig. 36.- The basal conglomerate of the Triassic succession at Campumari at stop 8.2 (alternative).

Stop 8.2: -The Sardinic unconformity, along the coast southwards from the Masua harbour

From Masua harbour we walk (20 minutes) along the cliff where the “Sardinic Unconformity” is sharp and exceptionally exposed. In this outcrop, the unconformity between the upper part of the Cabitza Formation (Middle Cambrian-Lower Ordovician), there made of anchimetamorphic siltstones, and the basal conglomerate of Monte Argentu Formation (Upper Ordovician) is quite at high angle (Fig. 37 and 38).

The clasts of the conglomerate are strongly variable in size; their composition reflects that of the underlying formations. The clasts are strongly flattened, according to the cleavage of the main Variscan phase (striking N-S), which also deforms the contact of the unconformity.



Fig. 38 -Detail of Fig 37, note the high angle between the unconformity (arrow) and the bedding (S_0 , solid line) in the Cabitza Fm. (Cab); the S_1 (dashed line) crosscuts the unconformity.



Fig. 37 -The Sardinic unconformity south of the Masua harbour, the square indicates the following figure; see location in Fig. 37.

The N-S trending folds, with step axial immersion, interfere with upright E-W trending folds related to the “Sardinic Phase”.

A detailed structural field mapping was carried out by Lebit (1996, Fig. 39). Measuring the strain of the Upper Ordovician pebbles he restored the unconformity section and highlighted the angle between the Sardinic unconformity and the bedding in the pre-Sardinic formation.

Here and in the coast just in front of this outcrop is possible to watch the superposition between the Sardinic folds, E-W trending, without an axial plane cleavage, and the Variscan, N-S trending folds, with a well-developed axial plane cleavage (Fig. 40).



Fig. 40.- E-W trending, fold (AxS) crosscut by the cleavage (S_v) related to the Variscan N-S trending folds, affecting the siltstones of the Cabitza Fm. In the right side of the picture the hinge of the E-W fold. Coast west of the Masua harbour, see location in Fig. 34.

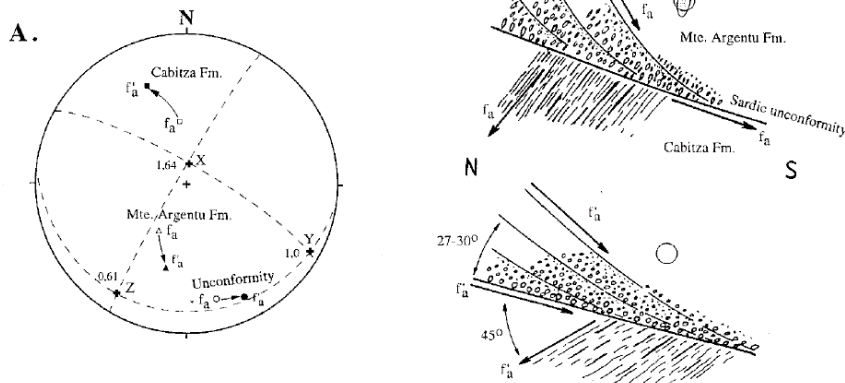


Fig. 39.- Restoration of the initial geometries of the Sardinic unconformity at the stop 8.2 (after Lebit, 1995 Ph.D. thesis).

References

- Arthaud F. (1963) - Un exemple de tectonique superposés dans le Paléozoïque de l'Iglesiente (Sardaigne). *C. R. Soc. Geol. France*, **9**, 303-304, Paris.
- Arthaud F. (1970) - Étude tectonique et microtectonique comparée de deux domaines Hercyniens: Les nappes de la Montagne Noire (France) et l'anticlinorium de l'Iglesiente (Sardaigne), Publications de l'Université des Sciences et Techniques du Languedoc - Série Géologie Structurale, 1, p. 175, Montpellier.
- Barca S., Ferretti A., Massa P., Serpagli E. (1992) - Minor Tectonic units within the Hercynian Arburese Nappe in Southwestern Sardinia. New structural and stratigraphic evidences. In: Carmignani L., Sassi F.P. (Eds.), Contribution to the Geology of Italy with special regard to the Paleozoic basement. A volume dedicated to Tommaso Coccozza. IGCP Project No. 276, Newsletter, 5, 51-55, Siena.
- Barca S., Olivieri R. (1991) - Age and source of calcareous blocks resedimented into Hercynian flysch type sediments of Sarrabus (southeastern Sardinia). *Atti Soc. Nat. Mat. Modena*, **122**, 49-66.
- Barca S., Costamagna L.G. (2003) - Analisi di facies e stratigrafia della successione permo?-triassica di Campumari-Coremò (Iglesiente, Sardegna SW). *Boll. Soc. Geol. It.*, **122**, 25-45.
- Bechstadt T., Boni M. (1994) - Sedimentological, stratigraphical and ore deposits field guide of the autochthonous cambro-ordovician of southern Sardinia, *Memorie Descrittive della Carta Geologica d'Italia*, **48**, p. 434. Roma.
- Calvino F. (1959) - Lineamenti strutturali del Sarrabus-Gerrei (Sardegna sudorientale). *Bollettino del Servizio Geologico d'Italia*, **81** (4-5), 489-556.
- Calvino F., 1960 - Lineamenti strutturali del Sarrabus-Gerrei (Sardegna sud-orientale). *Bollettino del Servizio Geologico d'Italia*, **81**, 489-556.
- Cappelli B., Carmignani L., Castorina F., Di Pisa A., Oggiano G., Petrini R. (1992) - A Variscan suture zone in Sardinia: geological and geochemical evidence, Paleozoic Orogenies in Europe special issue), *Geodin. Acta*, **5** (1-2), 101-118.
- Carmignani L., Oggiano G., Funedda A., Conti P., Pasci S., Barca S. (2008) - Geological map of Sardinia at 1:250,000 scale. Lac, Firenze.
- Casini L., Oggiano G. (2008) - Late orogenic collapse and thermal doming in the northern Gondwana margin incorporated in the Variscan Chain: a case study from the Ozieri Metamorphic Complex, northern Sardinia, Italy. *Gondwana Research*, Vol. 13 (3), p. 396-406. ISSN 1342-937X.
- Carmignani L., Barca S., Cappelli B., Di Pisa A., Gattiglio M., Oggiano G., Pertusati P.C. (1992) - A tentative geodynamic model for the Hercynian basement of Sardinia. In: Carmignani L. & Sassi F.P. (Eds.), Contribution to the Geology of Italy with special regard to the Paleozoic basement. A volume dedicated to Tommaso Coccozza. IGCP Project No. 276, Newsletter, 5, 61-82, Siena.
- Carmignani L., Barca S., Disperati L., Fantozzi P., Funedda A., Oggiano G., Pasci S. (1994) - Tertiary compression and extension in the Sardinian basement. *Boll. Geof. Teor. Appl.*, **36**, 45-62, Trieste.
- Carmignani L., Coccozza T., Minzoni N., Pertusati P.C. (1981) - Structural and palaeogeographic lineaments o the Variscan cycle in Sardinia. *Geol. Mijnbouw*, **60**, 171-181, Amsterdam.
- Carmignani L., Coccozza T., Minzoni N., Pertusati P.C. & Ricci C.A. (1979) - E' la Corsica il retro paese della catena ercinica della Sardegna? *Mem. Soc. Geol. It.*, **20**, 47-55, Roma.
- Carmignani L., Conti P., Pertusati P.C., Barca S., Cerbai N., Eltrudis A., Funedda A., Oggiano G., e Patta E.D. (2001a) - Note illustrative della Carta Geologica d'Italia alla scala 1:50.000. Foglio 549, Muravera, p. 13-21.
- Carmignani L., Pertusati, P.C. (1977) - Analisi strutturale di un segmento della catena ercinica: il Gerrei (Sardegna sud-orientale). *Bollettino della Società Geologica Italiana*, **96**, 339-364.
- Carmignani L., Coccozza T., Ghezzi C., Pertusati P.C., Ricci C.A. (1986) - Guide-book to the Excursion on the Paleozoic Basement of Sardinia. IGCP Project N. 5, Newsletter, special issue, 102 p.
- Carmignani L., Cortecchi G., Dessau G., Duchi G., Oggiano G., Pertusati P., Saitta M. (1978) - The antimony and tungsten deposit of Villasalto in South-Eastern Sardinia and its relationship with Hercynian tectonics. *Schweizerische Mineralogische und Petrographische Mitteilungen*, **58**, 163-188.
- Carosi R., Di Pisa A., Iacopini D., Montomoli C., Oggiano G. (2004) - The structural evolution of the Asinara Island (NW Sardinia, Italy). *Geodinamica Acta* 17/5 (2004) 309-329.
- Carosi R., Frassi C., Montomoli C. (2009) - Deformation during exhumation of medium- and high-grade metamorphic rocks in the Variscan chain in northern Sardinia (Italy). *Geological Journal*, **44** (2009), pp. 280-305
- Carosi R., Montomoli C., Tiepolo M., Frassi C. (2011). Geochronological constrains on post-collisional shear zones in the variscides of Sardinia (Italy). *Terranova*. Volume 24, Issue 1, pages 42-51, February 2012. DOI: 10.1111/j.1365-3121.2011.01035.
- Casini L., Senserini P., Oggiano G. (2009) - Evidence for water-assisted diffusional creep in the mylonite gneisses of Giuncana, northern Sardinia, Italy. *Trabajos de Geologia*, Universidad de Oviedo, **29**: 173-179.
- Casini L., Funedda A., Oggiano G. (2010) - A Balanced foreland-hinterland deformation model for the Southern Variscan belt of Sardinia, Italy. *Geological Journal*, Vol. 45 (5-6), p. 634-649. eISSN 1099-1034.
- Casini L., Cuccuru S., Maino M., Oggiano G. Tiepolo M. (2012) - Emplacement of the Arzachena Pluton (Corsica-Sardinia Batholith) and the geodynamics of incoming Pangaea. *Tectonophysics*, in press doi: 10.1016/j.tecto.2012.03.028.
- Cherchi G.P., Musumeci G. (1986) - Il leucogranite de M. Grighini (Sardegna centro-occidentale), un esempio di granito deformato all'interno di una fascia di taglio duttile: caratteristiche meso e microstrutturali. Atti della Società Toscana di Scienze Naturali Residente in Pisa, Memorie, Processi Verbali, Serie A ISSN 0365-7655 1986, vol. 93, p. 13-29 (16 ref.).
- Conti P., Carmignani L., Oggiano G., Funedda A., Eltrudis A. (1999) - From thickening to extension in the Variscan belt - kinematic evidence from Sardinia (Italy). *Terra Nova* Volume 11, Issue 2-3, pages 93-99, April/June 1999.
- Conti P., Funedda A. e Cerbai N. (1998) - Mylonite development in the Hercynian basement of Sardinia (Italy). *Journal of Structural Geology*, vol. 20, n° 2/3, 121-133, Oxford.
- Conti P., Patta E.D. (1998) - Large scale W-directed tectonics in southeastern Sardinia. *Geodinamica Acta*, **11** (4).
- Conti P., Carmignani L., Funedda A. (2001) - Change of nappe transport direction during the Variscan collisional evolution of central-southern Sardinia (Italy). *Tectonophysics*, v. 332, p. 255-273.
- Conti P., Funedda A., Cerbai N. (1998) - Mylonite development in the Hercynian basement of Sardinia (Italy). *Journal of Structural Geology*, **20** (2/3): 121-133.
- Cortesogno L., Gaggero L., Oggiano G., Paquette J.L. (2004) - Different tectono-thermal evolutionary paths in eclogitic rocks from the axial zone of the Variscan Chain in Sardinia (Italy) compared with the Ligurian Alps. *Ofoliti* **29** (2):125-144.
- Cruciani G., Franceschelli M., Elter F.M., Puxeddu M., Utzeri D. (2008b) - Petrogenesis of Al-silicate-bearing trondhjemitic migmatites from NE Sardinia, Italy. *Lithos*, **102**, 554-574.
- Cruciani G., Franceschelli M., Jung S., Puxeddu M., Utzeri D. (2008a) - Amphibole-bearing migmatite from Variscan Belt of NE Sardinia, Italy: partial melting of a mid-Ordovician igneous source. *Lithos*, **102**, 208-224
- Del Moro A., Di Simplicito P., Ghezzi C. Guasparri G., Rita F., Sabatini G. (1975) - Radiometric data and intrusive sequence in the Sardinian Batholith. *N. Jb. Mineral. Abh.*: **126**, 28-44, Stuttgart.

- Di Vincenzo G., Carosi R., Palmeri R. (2004) - The relationship between tectono-metamorphic evolution and argon isotope records in white mica: constraints from in situ ^{40}Ar - ^{39}Ar laser analysis of the Variscan basement of Sardinia. *Jour. Petr.*, **45**, 1013-1043.
- Di Pisa A., Oggiano G., Talarico F. (1993) - Post collisional tectono-metamorphic evolution in the axial zone of the Hercynian belt in Sardinia: the example from the Asinara island. Orleans, Doc. BRGM **219** (1993), 216-217.
- Dunnet D., Monnet J.M.M. (1969) - Inhomogeneous strain and the remobilization of ores and minerals. "Meeting on Remobilization of Ore and Minerals", Cagliari, 81-100.
- Ferrara G., Ricci C.A., Rita F. (1978) - Isotopic ages and tectono-metamorphic history of the metamorphic basement of north-eastern Sardinia. *Contr. Min. Petr.*, **68**, 99-106, Berlin.
- Ferré E.C., Leake B.E. (2001) - Geodynamic significance of early orogenic high-K crustal and mantle melts: example of the Corsica Batholith. *Lithos*, **59**, 47-67.
- Frassi C., Carosi R., Montomoli C., Law R.D. (2009) - Kinematics and vorticity of ?ow associated with post-collisional oblique transpression in the Variscan Inner Zone of northern Sardinia (Italy). *Journal of Structural Geology* **31**, 1458-1471.
- Funedda A., Carmignani L., Pertusati P.C., Forci A., Calzia P., Marongiu F., Pisano G., Serra M. -in stampa-F° 548 «Senorbi». Note illustrative della carta geologica d'Italia in scala 1:50.000. Bozze approvate per la stampa, ISPRA-Servizio Geologico d'Italia, Roma.
- Gaggero L., Oggiano G., Buzzi L., Slejko F. and Cortesogno L. (2007) - Post-Variscan mafic dykes from the late orogenic collapse to the Tethyan rift: evidence from Sardinia, *Ophioliti* **32** (2007) 15-37.
- Giacomini F., Bomparola R., Ghezzi C., Gulbrandsen H. (2006) - The geodynamic evolution of the Southern European Variscides: constraints from the U/Pb geochronology and geochemistry of the lower Palaeozoic magmatic-sedimentary sequences of Sardinia (Italy). *Contrib. Mineral. Petrol.*, **152**, 19-24.
- Giacomini F., Bomparola R.M., Ghezzi C. (2005) - Petrology and geochronology of metabasites with eclogite facies relics from NE Sardinia: constraints for the Palaeozoic evolution of Southern Europe. *Lithos*, **82**, p. 221-248.
- Giacomini F., Dallai L., Carminati E., Tiepolo M., Ghezzi C. (2008) - Exhumation of a Variscan orogenic complex: insights into the composite granulitic-amphibolitic metamorphic basement of south-east Corsica (France). *Journal of Metamorphic Geology*. Volume 26, Issue 4, pages 403-436, May 2008.
- Kruhl J.H., Vernon, R.S. (2005) - Syndeformational emplacement of a tonalitic sheet complex in a late-Variscan thrust regime: fabrics and mechanism of intrusion, Monte'e Senes, northeastern Sardinia, Can. Min. **43** (2005) 387-407.
- Kruhl J.H., Vernon R.S. (2005) - Syndeformational emplacement of a tonalitic sheet complex in a late-Variscan thrust regime: fabrics and mechanism of intrusion, Monte'e Senes, northeastern Sardinia, Can. Min. **43** (2005) 387-407.
- Lebit H. (1995) - On fold and strain interference patterns in the Paleozoic rocks of Iglesias (SW Sardinia). PhD. thesis, ETH Zürich.
- Leone F., Hamman W., Laske R., Serpagli E., Villas E. (1991) - Lithostratigraphic units and biostratigraphy of the post-sardic Ordovician sequence in south-west Sardinia. *Boll. Soc. Paleont. It.*, **30**, 201-235, Modena.
- Leone F., Loi A., Pillola G.L. (1995) - The post-sardic Ordovician sequence in south-western Sardinia. In: Cherchi A. (Ed.), 6th Paleobenthos International Symposium, Guide-Book. Cagliari, October 25-31, 1995. Rend.Sem Fac. Sc. Univ. Cagliari (suppl. Vol. 65): 81-106, Cagliari.
- Macera P., Di Pisa A., Gasperini D. (2011) - Geochemical and Sr-Nd isotope disequilibria during multi-stage anatexis in a metasedimentary Hercynian crust., *European Journal of Mineralogy: an International Journal of Mineralogy, Geochemistry and related Sciences*, vol. 23, p. 207, tot. pag 16, tot. autori 3, 2011.
- Maxia M. (1983) - Segnalazione di potenti successioni carbonatifere marine nella Sardegna meridionale. *Rend. Soc. Geol. It.*, **6**, 21-24, Roma.
- Oggiano G., Di Pisa A. (1988) - I graniti peralluminosi sin-tettonici ell'area di Trinità d'Agultu e i loro rapporti con le metamorfite di alto grado della Bassa Gallura (Sardegna settentrionale). *Boll. Soc. Geol. It.*, **107**, 471-480.
- Oggiano G., Gaggero L., Funedda A., Buzzi L., Tiepolo M. (2010) - Multiple early Paleozoic volcanic events at the northern Gondwana margin: U-Pb age evidence from the Southern Variscan branch (Sardinia, Italy). *Gondwana Research*, **17** (2010), p. 44-58
- Oggiano G., Casini L., Rossi P., Mameli P. (2007) - Long lived dextral strike-slip tectonics in in the southern Variscan Belt: evidence from two syn-kinematic intrusions in north Sardinia. *Geologie de la France (Meeting on Mechanics of Variscan Orogeny: a modern view on orogenic research Orleans 13-15 2007)*, **2**, 141.
- Oggiano G., Cherchi G.P., Aversano A., Di Pisa A., Ulzega A., Orrù P., Pintus C. (2005) - Note illustrative della Carta Geologica d'Italia, Foglio 428 Arzachena. Firenze: S.EL.CA.
- Palmeri R., Fanning M., Franceschelli M., Memmi I., Ricci C.A. (2004) - Shrimp dating of zircons in eclogite from the Hercynian basement from north eastern Sardinia (Italy). *Neus Jahrbuch. Fur Mineralogie Monatshefte* **6**, 275-288.
- Paquette J.-L., Ménot R.-P., Pin C., Orsini J.-B. (2003) - Episodic short-lived granitic pulses in a post-collisional setting: evidence from precise U-Pb zircon dating through a crustal cross-section in Corsica, *Chem. Geol.*, **198** (2003) 1-20.
- Pavanetto P., Funedda A., Northrup C.J., Schmitz M., Crowley J., Loi A. (2012) - Structure and U-Pb zircon geochronology in the Variscan foreland of SW Sardinia, Italy. *Geological Journal*.
- Pillola G.L. (1991). Trilobites du Cambrien inférieur du SW de la Sardaigne, Italie. *Paleontol. Ital.*, **78**, 1-173, Pisa.
- Pittau P., Del Rio M & Funedda A. (2008) - Relationships between plant communities characterization and basin formation in the Carboniferous-Permian of Sardinia. *Boll. Soc. Geol. It. (Ital.J.Geosci.)*, **127** (3), 637-653.
- Poli G., Tommasini S. (1999) - Insights on acid-basic magma interaction from the Sardinia-Corsica batholith: the case study of Sarrabus, southeastern Sardinia, Italy. *Lithos*, **46** (3), 553-571.
- Poll J.J.K., Zwart H.J. (1964) - On the tectonics of the Sulcis area, S Sardinia. *Geol. Mijnbouw*, **43**, 144-146, Amsterdam.
- Poll J.J.K. (1966) - The geology of the Rosas-Terreseo area, Sulcis, South Sardinia. *Leidse Geol. Med.*: **35**, 117-208, Leyden.
- Rossi P., Cocherie A. (1991) - Genesis of a Variscan batholith. Field, petrological and mineralogical evidence from the Corsica-Sardinia batholith, in: Freeman R., Huch M., Mueller St. (Eds) The European Geotraverse part 7, *Tectonophysics*, **195**, 319-346.
- Rossi P., Durand-Delga M., Cocherie A. (1993) - Caractère volcano-plutonique du magmatisme calco-alcalin composite d'âge Stéphanien supérieur-Permien inférieur en Corse. *C. R. Acad. Sci. Paris, Série II*: p. 1779-1788, Paris.
- Rossi Ph., Oggiano G., Cocherie A. (2009) - A restored section of the 'southern Variscan Realm' across the Corsica-Sardinia microcontinent. *C. R. Geosc.*, **341**, 224-238.
- Stille H. (1939) - Bemerkungen betreffend die <<Sardische>> Faultung und den Ausdruck <<Ophiolitisch>>. *Zs. Deutsc. Geol. Ges.*, **91**, 771-773.
- Teichmüller R. (1931) - Zur Geologie des Thyrrhenisgebietes. Teil 1: Alte und junge Krustenbewegungen im südlichen Sardinien. Abhandlungen von der Gesellschaft der Wissenschaften zu Göttingen, Mathematisch-Physikalische Klasse, **3** (3): 857-950.

SCIENTIFIC PROGRAMME

22 – 23 May